Stochastic Economic Model Predictive Control for Trading Energy and Ancillary Services with Storage

Luca Santosuosso, Simon Camal, Francesco Liberati, Alessandro Di Giorgio, Andrea Michiorri, Georges Kariniotakis

▶ **To cite this version:**

Luca Santosuosso, Simon Camal, Francesco Liberati, Alessandro Di Giorgio, Andrea Michiorri, et al.. Stochastic Economic Model Predictive Control for Trading Energy and Ancillary Services with Storage. Sustainable Energy, Grids and Networks, 2024, pp.101373. 10.1016/j.segan.2024.101373 . hal-03641708

HAL Id: hal-03641708

https://minesparis-psl.hal.science/hal-03641708

Submitted on 4 Apr 2024

HAL is a multi-disciplinary open access archive for the deposit and dissemination of scientific research documents, whether they are published or not. The documents may come from teaching and research institutions in France or abroad, or from public or private research centers.

L'archive ouverte pluridisciplinaire **HAL**, est destinée au dépôt et à la diffusion de documents scientifiques de niveau recherche, publiés ou non, émanant des établissements d'enseignement et de recherche français ou étrangers, des laboratoires publics ou privés.

Stochastic Economic Model Predictive Control for Renewable Energy and Ancillary Services Trading with Storage

Luca Santosuosso[a], Simon Camal[a], Francesco Liberati[b], Alessandro Di Giorgio[b], Andrea Michiorri[a], Georges Kariniotakis[a]

[a]*MINES Paris - PSL University, Centre for Processes, Renewable Energies and Energy Systems (PERSEE), 1 rue Claude Daunesse, Sophia Antipolis, 06904, , France*
[b]*DIAG Department of the Sapienza University of Rome, Via Ariosto 25, Rome, 00185, , Italy*

Abstract

The provision of renewable-based ancillary services (AS) is paramount for the stable operation of power systems featuring high renewable penetration. The combined operation of storage with renewables enables aggregators to increase the reliability of their energy and frequency-control AS offers. Existing dispatch strategies for the supply of both energy and AS are usually rule-based or involve tracking a technical reference signal, hence economically suboptimal for aggregators. This study proposes a comprehensive decision framework in which first a stochastic optimization derives bids on energy and AS markets, then stochastic economic Model Predictive Control (SEMPC) optimizes the dispatch of the storage in order to maximize the profit and minimize the storage degradation, as a function of the predicted renewable production and the expected AS activation.

The framework is applied to a real-world case study where storage combined with wind power participates in the energy market, the frequency containment market and the frequency restoration reserve market. The SEMPC-based approach increases market revenue by 15% compared to a standard reference tracking MPC, and reduces storage degradation by 23%. The stochastic formulation lowers the sensitivity of the economic objectives to renewable energy forecast errors, compared to deterministic approaches.

Keywords:
stochastic economic model predictive control, ancillary services, frequency control, stochastic programming, renewable energy, storage degradation

Acronyms

aFRR automatic Frequency Restoration Reserve.

AS Ancillary Services.

BASMP Balancing Ancillary Services Market Penalty.

BASMR Balancing Ancillary Services Market Remuneration.

BESS Battery Energy Storage System.

BRP Balancing Responsible Party.

BSP Balancing Service Provider.

DA Day Ahead.

DAM Day Ahead Market.

DDA Deterministic Day Ahead.

DEMPC Deterministic Economic Model Predictive Control.

DRTMPC Deterministic Reference Tracking Model Predictive Control.

EMPC Economic Model Predictive Control.

FCR Frequency Containment Reserve.

GCT Gate Closure Time.

MPC Model Predictive Control.

PFR Primary Frequency Regulation.

RTMPC Reference Tracking Model Predictive Control.

SDA Stochastic Day Ahead.

SEMPC Stochastic Economic Model Predictive Control.

SFR Secondary Frequency Regulation.

SMPC Stochastic Model Predictive Control.

SoC State of Charge.

ST Short Term.

TSO Transmission System Operator.

vRES variable Renewable Energy Sources.

1. Introduction

In order to mitigate climate change and cope with the massive increase of energy demand all over the world, the energy sector is called to speed up the decarbonization of the energy system. Renewable technologies, which currently provide around 30% of electricity generation, are therefore set for a rapid growth in the near future [1].

The increasing penetration of variable Renewable Energy Sources (vRES) creates a trend towards higher imbalances between energy generation and consumption in power systems, due to vRES energy forecast errors. Additionally, conventional generators tend to be replaced by vRES in the generation portfolio. To ensure safe grid operation under high vRES penetration, new technologies should offer reserve capacities in the existing markets for balancing ancillary services (AS) [2]. An example of such newcomers in the provision of balancing AS is Battery Energy Storage Systems (BESSs). Their fast response and ability to provide symmetrical reserve (upward and downward regulation of active power) have led to the successful entry of BESSs in markets for primary frequency regulation (PFR) in the USA [3] and Europe, where this service is called Frequency Containment Reserve (FCR) [4]. Energy-intensive services such as secondary frequency regulation (SFR), also called automatic Frequency Restoration Reserve (aFRR) in the European terminology, are challenging for BESSs, because they require more energy throughput from storage than PFR and therefore accelerate storage degradation. It is easier for BESSs to provide multiple balancing AS, e.g., PFR and SFR, if they are integrated into larger pools, such as the portfolio of an aggregator integrating vRES plants [5]. This enables the variability of vRES production to be mitigated within the perimeter of the aggregator [6], and part of this portfolio to be dedicated to the supply of balancing AS jointly optimized with the production of energy. Examples of the coordinated operation of vRES and storage can be found in hybrid systems. These systems combine vRES and BESS under the same grid connection point, so that the BESS can directly compensate vRES energy forecast errors [7] and derive market offers that coordinate the expected vRES production with the BESS capacity [8].

In this context, the provision of energy and multiple frequency-control AS through a combination of renewables and storage is an interesting research topic with respect to two main challenges. The first challenge involves optimizing the two-step decision chain composed of (1) trading (in all considered markets) and (2) control of the vRES+storage combination, in order to maximize value (trading profit and storage lifetime) and compensate imbalances. This requires a comprehensive modeling of the multiple AS and of the storage degradation in both the trading and control phases. In the existing literature, this modeling is generally lacking or else incomplete in one of the two phases of the decision chain. The second challenge concerns the uncertainty of vRES production, which must be integrated into the optimization approach because the BESS size is limited due to high investment costs, therefore imbalances are expected to occur between the contracted and delivered volumes. An appropriate stochastic formulation for the entire decision chain appears necessary to mitigate the impact of vRES energy forecast errors on the profitability of the vRES+BESS system.

1.1. Literature review

The optimization of vRES participation in the electricity markets is an established research field. In order to maximize the expected profit and minimize the risk of exposure to high financial

loss, researchers have identified the importance of correctly modeling uncertainties concerning renewable production or market conditions. Approaches to date have focused mainly on the energy market, and cover a large spectrum of solutions ranging from stochastic optimization [9] and robust optimization [10], to hybrid stochastic/robust optimization models [11] and other alternative approaches. In particular, [12] replaces the traditional predict and optimize chain with a single step based on prescriptive trees. The chance-constrained optimization proposed by [13] addresses joint trading in energy and balancing AS markets, but focuses on renewable-based aggregations without storage capacities. In [14], an integrated approach is proposed to optimize the offering strategy of a wind+storage system and derive real-time operation policies based on Linear Decision Rules, but participation in AS markets is neglected. Overall, methods exist to mitigate the impact of uncertainties on trading decisions for the energy market, but no adaptation has been proposed for the complex use case where balancing AS are integrated into the trading and control of vRES coupled with storage.

The provision of AS through the utilization of vRES and storage has garnered considerable attention in recent literature.In [15], a physics-based model is proposed the provision of PFR and voltage control by electric vehicles. In [16], a two-level optimization-based strategy is proposed for the provision of aFRR using a variable speed pump storage. In [17], a state-machine-based coordinated control strategy is presented for hybrid wind-BESS provision of frequency-control AS at different timescales, namely PFR and SFR activated through Automatic Generation Control. In [18], rule-based strategies are employed for the participation of PV with storage in secondary reserve markets. These works provide realistic modeling of the mechanisms for reserve procurement and activation, but do not consider the value of updated forecasts at intraday horizons to optimize the control of the vRES+BESS system.

The activation of balancing AS is performed almost instantaneously in real-time [19]. Thus, fast online control strategies are required to meet the system need of AS in real-time. Model Predictive Control (MPC) is an online optimization-based control method that adjusts the control strategies at every time-step based on the current information and a prediction of the future information [20]. The traditional reference-tracking MPC (RTMPC) is the most common MPC strategy employed in power system applications. This strategy follows a hierarchical approach where an upper-level problem derives one or several reference set-points, while at the lower level, the RTMPC controls the system to minimize the deviation between the controlled variables and the reference set-points. This two-level control approach is utilized in [21] for the participation of vRES-BESS hybrid systems in energy and ancillary services markets. First, a bidding strategy is formulated as a mixed-integer linear program. Second, RTMPC is employed to minimize deviations from the original schedule. RTMPC is used in [22] for the SFR of microgrids operated in islanded mode under cyberattacks. However, despite the effectiveness of this approach in tracking real-time activation of AS, control strategies involving RTMPC may not provide optimal solutions when coming to energy and AS trading problems. In fact, there is no guarantee that such hierarchical control approaches would optimize the economic objectives of the aggregator.

To overcome this issue, a new trend has emerged in the design of predictive controllers for economic-oriented problems, known as economic MPC (EMPC) [23], which directly optimizes the economic value of the system. In [24], EMPC is used for hydrogen-based microgrid energy trading in multiple electricity markets, including the balancing AS market. In [25], an EMPC ap-

proach is presented for microgrid participation in the spinning reserve AS market. A combination of Lasso MPC for PFR and EMPC for SFR is proposed in [26], for the case of virtual power plant energy and AS trading. In [27] EMPC is applied alongside a seasonal-autoregressive-integral-moving-average prediction model, enabling the participation of electric vehicles in the AS market for frequency regulation. In [28], a myopic controller is extended by introducing an improved EMPC for the participation of vRES-BESS in energy and ancillary services markets. Despite the appealing properties that EMPC demonstrates when dealing with market-based problems, it insufficiently models the uncertainties associated to vRES production and market quantities.

To hedge against the impact of uncertainties in the control strategy, stochastic MPC (SMPC) [29] is often used, which results from the application of stochastic programming to MPC. This control approach typically considers either chance constraints or scenarios. Chance-constraint-based SMPC methods set a specific level of probability that a constraint will be satisfied, while in scenario-based SMPC approaches the uncertainties are modeled with scenarios of possible realizations. Scenario-based SMPC approaches provide an effective solution to handle bounded uncertainties, while chance-constraint-based SMPC methods are typically recommended in case of unbounded uncertainties. Several applications of SMPC to microgrid energy management problems can be found in the literature. In [30], a two-level stochastic framework is introduced for optimizing microgrid participation in the day-ahead market (DAM) and the provision of regulation capacity. The proposed SMPC strategy is designed to reschedule the initial planning based on the system requirements of AS. In [31] a scenario-based SMPC strategy is proposed to minimize microgrid operational costs and emissions. An interesting application of SMPC can be found in [32] for the energy management problem of a hybrid PV-EV system considering PV generation, EV consumption and market prices as sources of uncertainty. To reduce the computational effort, an offline solution to the SMPC problem is computed via multiparametric programming and then used to operate the system in real-time.

However, despite the noticeable interest for the ideas of SMPC and EMPC, very few attempts have been made to account for both system uncertainties and economic-oriented objectives in the design of predictive controllers for energy and AS trading problems. Such a MPC strategy arises from the combination of EMPC and SMPC, and is known in the literature as stochastic economic MPC (SEMPC). An example is given in [33], which features a scenario-based SEMPC strategy for the energy trading of a hybrid PV-BESS system. In [34], SEMPC is applied to the energy management problem of residential microgrids. Based on load, weather and price forecasts, a fully stochastic two-level architecture is proposed to trade energy on the DAM and minimize imbalances in real-time by means of SEMPC. In [35], real-time deviations of a market participant from its original schedule are minimized using a sample-based SEMPC strategy to handle wind power generation uncertainty. Similarly, in [36], small-size controllable loads participating in a demand response program are used to trade energy on the DAM, and a SEMPC strategy is proposed to compensate the aggregator imbalances on the intraday market. However, none of these studies involve participating in the AS markets.

1.2. Research gaps and contributions

From the literature analysis, several gaps can be identified in the current state of the art. Various ideas have been applied to problems involving energy trading and AS provision, such as rule-based

strategies [18], physics-based models [15], state-machine-based control [17] and optimization-based strategies [16, 37]. Compared to these approaches, predictive control can significantly enhance control performances through the integration of updated predictions on future information. However, in most of the proposed applications of predictive control, traditional RTMPC strategies are proposed to tackle control problems, like in [22, 30]. In these studies, market participation is often overlooked, or the controller does not explicitly consider economic key performance indicators in the objective function. When MPC is used to tackle trading problems, the proposed strategies employ deterministic models, like in [24, 25, 26, 27], and are thus unable to hedge against the impact of various sources of uncertainty. In the few cases in which predictive controllers are designed to consider both stochastic models and economic objectives, either the problem does not involve trading, like in [32], or only energy trading is considered and participation in the AS market is neglected, like in [33, 34, 35, 36].

To the best of the authors' knowledge, a multi-timescale fully stochastic architecture employing SEMPC for renewable energy and AS trading with storage is missing. Therefore, the main contributions of this paper compared to the related literature could be summarized as follows:

- A two-level architecture is proposed for trading energy and providing frequency-control AS through predictive control, whereas existing works focus only on the energy market [33, 34, 35, 36] or employ simple strategies (e.g., rule-based [18], state-machine-based [17]) to participate in AS markets.
- The model chain is fully stochastic, composed of scenario-based stochastic programming for the trading phase and scenario-based SEMPC for real-time control. Thus, the proposed architecture hedges against the impact of significant vRES energy forecast errors throughout the decision chain from trading to control, whereas existing works involving MPC employ deterministic models [24, 25, 26].
- The proposed SEMPC strategy optimizes both storage dispatch and market participation near to real-time, resulting in higher market revenue and lower storage degradation compared to traditional RTMPC, as, in, e.g., [30].

Moreover, real-world data from the European H2020 project Smart4RES [38] have been used to validate the effectiveness of the proposed method. Table 1 provides a comparison between this work and the relevant related literature.

The remainder of the article is organized as follows. Section 2 describes the data, the models, the proposed trading and control strategy, and the benchmarks used to evaluate our novel approach. Section 3 presents the case study and the simulation results. Finally, Section 5 concludes this study.

2. Methodology

In this section, the discussion revolves around the modeling and methods proposed to address various time steps inherent in the current problem. First, the modeling of the energy and balancing AS market mechanism, the activation of balancing energy, and storage degradation is presented. Subsequently, a novel two-level stochastic architecture for day-ahead (DA) trading and short-term

Ref.	Energy market	AS market	AS provision	Trading strategy	Control strategy
[9]	✓	×	×	Stochastic programming	×
[10]	✓	×	×	Robust optimization	×
[11]	✓	×	×	Hybrid stochastic/robust optimization	×
[12]	✓	×	×	Prescriptive trees	×
[15]	×	×	Frequency and voltage regulation	×	Physic-based
[17]	×	✓	Frequency regulation	×	State-machine-based
[18]	✓	✓	Frequency regulation	Linear programming	Rule-based
[21]	✓	✓	Frequency regulation	Mixed-integer linear programming	RTMPC
[22]	×	×	Frequency regulation	×	RTMPC
[25]	×	✓	Spinning reserve	×	EMPC
[27]	×	✓	Frequency regulation	×	EMPC
[30]	✓	✓	Flexibility services	Stochastic programming	SMPC
[33]	✓	×	×	×	SEMPC
[34]	✓	×	×	Stochastic programming	SEMPC
[35]	✓	×	×	×	SEMPC
[36]	✓	×	×	×	SEMPC
This study	✓	✓	Frequency regulation	Stochastic programming	SEMPC

Table 1: Summary of the relevant related research.

(ST) control of the hybrid system is introduced. Lastly, for the sake of comparison, two benchmark approaches, alternative to our architecture, are briefly outlined.

2.1. Notation

In the following, discrete time problems are presented over a finite set of sampling times $t \in T$ with a sampling period of Δ_t. The subscript t is used to indicate that a variable or a parameter

is associated to the sampling time t, e.g., x_t. Functions of the decision variables and vectors are denoted in **bold**. The cardinality of a set, e.g., T, is denoted with the symbol $|\cdot|$, e.g., $|T|$.

Nomenclature

Superscripts and subscripts:

^{DA} Superscript to denote variables and parameters associated with the DA step.

ST Superscript to denote variables and parameters associated with the ST step.

$_{\tau|t}$ Subscript to denote the value of a variable computed at time t and referring to time τ.

Sets and indexes:

$\boldsymbol{z^{DA,II}}$ Set of second stage decision variables in the DA optimization problem.

$\boldsymbol{z^{DA,I}}$ Set of first stage decision variables in the DA optimization problem.

$\boldsymbol{z^{ST}}$ Set of decision variables in the ST control problem.

Ω Set of scenarios, index ω.

K Prediction horizon, index k.

T Set of time periods, index t.

Decision variables:

$\Delta E^{\uparrow/\downarrow}$ Negative/Positive energy imbalance [MWh].

$\Delta R^{FCR}, \Delta R^{aFRR,\uparrow/\downarrow}$ FCR deficit and upward/downward aFRR deficit [MW], respectively.

b^c, b^d Binary variables associated with BESS charging and discharging power [-], respectively.

E Energy offer in the DAM [MWh].

p^c, p^d BESS charging and discharging power [MW], respectively.

$R^{FCR}, R^{aFRR,\uparrow/\downarrow}$ FCR offer and upward/downward aFRR offer in the balancing AS market [MW], respectively.

x Energy stored in the BESS [MWh].

Symbols:

$\alpha^{FCR}, \alpha^{aFRR,\uparrow/\downarrow}$ FCR activation signal and upward/downward aFRR activation signal [-], respectively.

$\boldsymbol{\delta E^2}$ Quadratic term in RTMPC objective function, used to penalize energy imbalances [-].

$\boldsymbol{\delta R^2}$ Quadratic term in RTMPC objective function, used to penalize reserve deficits [-].

$\boldsymbol{cl}(\cdot), \boldsymbol{cy}(\cdot,\cdot)$ BESS calendar and cycling aging factors [MWh], respectively.

$\boldsymbol{D}(\cdot,\cdot)$ BESS degradation function [RON].

$\boldsymbol{eb^2}$ Quadratic term in RTMPC objective function, used to penalize deviations from DA BESS schedule [-].

$\boldsymbol{J^{DA}}, \boldsymbol{J^{ST}}$ Objective functions of the DA and ST optimization problems [RON], respectively.

$\boldsymbol{R^{aFRR,\alpha}}$ Net reserve volume activated for secondary frequency-control (aFRR) [MW].

$\boldsymbol{R^{FCR,\alpha}}$ Reserve volume activated for primary frequency-control (FCR) [MW].

Δ_t, Δ_k Duration of time period and control period [s], respectively.

η^c, η^d BESS charging and discharging efficiencies [-], respectively.

π^B Cost of a complete BESS charge/discharge cycle [RON/MWh].

π^E DAM energy price [RON/MWh].

$\pi^{\Delta R,aFRR,comp,\uparrow/\downarrow}$ Composite penalty price of upward/downward aFRR (formed by combining penalty prices of availability remuneration and activation remuneration) [RON/MW].

$\pi^{\Delta R,FCR}, \pi^{\Delta R,aFRR,\uparrow/\downarrow}$ Penalty prices of FCR deficit and upward/downward aFRR deficit [RON/MW], respectively.

$\pi^{aFRR,comp,\uparrow/\downarrow}$ Composite price of upward/downward aFRR (formed by combining prices of availability remuneration and activation remuneration) [RON/MW].

$\pi^{aFRR,bal,\uparrow/\downarrow}$ Price of activated upward/downward aFRR balancing energy [RON/MWh].

$\pi^{E,\uparrow/\downarrow}$ Penalty price of negative/positive energy imbalance [RON/MWh].

$\pi^{FCR}, \pi^{aFRR,\uparrow/\downarrow}$ Prices of FCR and upward/downward aFRR [RON/MW], respectively.

$p^{c,min/max}, p^{d,min/max}$ Min/Max BESS charging and discharging power [MW], respectively.

w_{cy}, w_{cl} Weights of BESS cycling and calendar aging [-], respectively.

x^i Energy stored in the BESS at the beginning of the simulation period [MWh].

$x^{cl,thr}$ Calendar aging threshold (above this energy level, the BESS is also affected by calendar aging) [MWh].

$x^{min/max}$ Min/Max BESS energy storage levels [MWh].

y Energy produced from vRES [MWh].

y^{max} vRES installed capacity [MW].

Vectors:

$\boldsymbol{\alpha}$ Vector of AS activation signals, encompassing both FCR and aFRR activation signals.

$\boldsymbol{\Delta E^{DA}}, \boldsymbol{\Delta E^{ST}}$ Vectors of DA and ST energy imbalances, respectively.

$\boldsymbol{\Delta R^{DA}}, \boldsymbol{\Delta R^{ST}}$ Vectors of DA and ST reserve deficits, respectively. These vectors encompass both FCR and aFRR deficits.

$\boldsymbol{\eta}$ Vector of BESS charging and discharging efficiencies.

$\boldsymbol{\pi^{R}}$ Vector of reserve prices, encompassing both FCR and aFRR unitary prices.

$\boldsymbol{\pi^{\Delta E}}$ Vector of energy imbalances penalty prices.

$\boldsymbol{\pi^{\Delta R}}$ Vector of reserve deficits penalty prices, encompassing both FCR and aFRR deficits prices.

$\boldsymbol{P^{DA}}, \boldsymbol{P^{ST}}$ Vectors of DA and ST BESS power commands, respectively.

$\boldsymbol{R^{DA}}$ Vector of reserve offers, encompassing both FCR and aFRR offers.

$\boldsymbol{u^{ST}}$ Sequence of ST control outputs.

2.2. Modeling

The following discusses the modeling of the energy market, the balancing AS market, and the BESS degradation. This study takes the perspective of an aggregator operating a hybrid vRES-BESS system on the wholesale electricity market to trade energy and frequency-control AS. The proposed models are based on the mechanisms currently implemented in Europe. However, a detailed description of the European electricity markets is beyond the scope of this study. For an extensive analysis of the recent evolution in the European electricity markets the reader can refer to [39], while detailed overviews are provided in [40] for the European AS markets and in [19] for the European balancing mechanism.

At present, the energy exchange in Europe takes place in several markets at different timescales [41]. All market participants, like the aggregator considered in this study, must keep their individual positions (sum of energy injected or withdrawn from the electrical grid) in balance, to help ensure the secure operation of the electrical grid; they are thus called Balancing Responsible Parties (BRPs) [19]. BRPs are subject to market penalties when they fail to keep their individual position in balance. Due to the uncertain nature of renewable power generation, an aggregator that includes vRES in its portfolio is likely to deviate from the schedule submitted to the market and thus face penalties as a consequence of its imbalances (deviations from the schedule submitted to the market). To minimize these penalties, the aggregator can exploit sources of flexibility (e.g., a BESS) to compensate in real-time the deviations from the original schedule. From a global perspective, some BRPs will have positive imbalances (energy surplus, i.e., more energy produced than originally scheduled), while others will have negative imbalances (energy shortage, i.e., less

energy produced than originally scheduled). Thus, the imbalances of all BRPs will partially cancel each other out. The remaining imbalance is cancelled through the frequency-control process, which employs balancing energy to restore the nominal frequency (50 Hz in Europe). Balancing energy is provided by Balancing Service Providers (BSPs) on specific markets, called balancing AS markets [19]. On these markets, BSPs offer upward and downward balancing capacities, which are called reserves, to the Transmission System Operator (TSO). In real-time, the TSO will eventually activate the reserves to restore the nominal frequency. The frequency-control process involves various steps, namely primary, secondary and tertiary control, employing different balancing products [19]. The nomenclature currently employed in the European balancing AS markets [19, 40] is adopted here. In particular, the focus is directed specifically towards two balancing products: **Frequency Containment Reserve** (**FCR**) for primary frequency-control and **automatic Frequency Restoration Reserve** (**aFRR**) for secondary frequency-control.

2.2.1. Energy market

Market participants submit energy bids on the market before the gate closure time (GCT), when the market session closes. In the DAM, sessions take place every day to trade energy for the following day. Thus, the GCT for the DAM is 24h before the actual energy injection time. In this context, the aggregator is assumed to offer energy volumes E in the DAM. The symbol π^E is used to denote the price associated with the energy exchange. As a BRP, the aggregator is financially responsible for its imbalances. In addressing penalties related to energy imbalances, a dual-price settlement scheme is assumed [42]. This scheme calculates separate prices for positive imbalances (actual energy injection exceeding the original energy offer) and negative imbalances (actual energy injection falling below the original energy offer). Thus, a penalty price $\pi^{E,\uparrow}$ is associated with negative imbalances $\Delta E^{\uparrow}$ while positive imbalances $\Delta E^{\downarrow}$ are rewarded with a price $\pi^{E,\downarrow}$ lower than π^E.

2.2.2. Balancing ancillary services market

The aggregator is also assumed to participate in the trading of balancing products, thus assuming the role of a BSP. On the balancing AS market, the aggregator offers upward reserve, which consists in offering energy capacity to increase the injection of energy into the grid, and a downward reserve, which consists in offering energy capacity to absorb energy from the grid. For primary frequency control, the aggregator offers FCR, denoted by R^{FCR}, while for secondary frequency control, the aggregator offers upward and downward aFRR, denoted by $R^{aFRR,\uparrow}$ and $R^{aFRR,\downarrow}$, respectively. FCR is modeled with a single variable since this product is assumed to be symmetric (the offer of upward reserve equals the offer of downward reserve), which is the case in many European balancing AS markets (e.g., Germany) [40].

Balancing energy is remunerated in two ways [42]: capacity remuneration, also known as availability remuneration; and energy remuneration, also known as activation remuneration. In the former case, the aggregator is remunerated to keep balancing capacity available for frequency-control. In the latter case, the aggregator is compensated for the actual activation of the balancing product. While both FCR and aFRR products receive a capacity remuneration, energy remuneration is only payed for the aFRR product.

The price of FCR is denoted by π^{FCR}, while the price of upward aFRR and downward aFRR are denoted by $\pi^{aFRR,\uparrow}$ and $\pi^{aFRR,\downarrow}$, respectively. Moreover, in addition to capacity prices, aFRR is also characterized by a price $\pi^{aFRR,bal,\uparrow}$ for activating upward aFRR balancing energy and a price $\pi^{aFRR,bal,\downarrow}$ for activating downward aFRR balancing energy.

The balancing capacity procured on the market can be activated in real-time during the frequency-control process. The activation of FCR is driven by the FCR activation signal $\alpha^{FCR} \in [-1, 1]$. When $\alpha^{FCR} > 0$, the BSP activates upward FCR (full activation when $\alpha^{FCR} = 1$). Conversely, if $\alpha^{FCR} < 0$, the BSP activates downward FCR (full activation when $\alpha^{FCR} = -1$).

Similarly, the activation of aFRR is driven by the aFRR activation signals. In this case, two activation signals are required to distinguish between the activation of upward and downward aFRR, which are denoted by $\alpha^{aFRR,\uparrow} \in [0, 1]$ and $\alpha^{aFRR,\downarrow} \in [0, 1]$, respectively. When $\alpha^{aFRR,\uparrow} > 0$, the BSP activates upward aFRR (full activation when $\alpha^{aFRR,\uparrow} = 1$). If $\alpha^{aFRR,\downarrow} > 0$, the BSP activates downward aFRR (full activation when $\alpha^{aFRR,\downarrow} = 1$).

It is assumed that activation signals are received by the aggregator from the TSO.

In light of the previous discussion on the balancing AS market and the activation mechanisms for balancing energy, the total compensation obtained by the aggregator in the balancing AS market, referred to as Balancing Ancillary Services Market Remuneration (BASMR), is expressed in Eq. (1).

$$\begin{aligned} \text{BASMR} = & \underbrace{\pi^{FCR} \cdot R^{FCR} + \pi^{aFRR,\uparrow} \cdot R^{aFRR,\uparrow} + \pi^{aFRR,\downarrow} \cdot R^{aFRR,\downarrow}}_{\text{availability remuneration}} + \\ & + \underbrace{\alpha^{aFRR,\uparrow} \cdot \pi^{aFRR,bal,\uparrow} \cdot R^{aFRR,\uparrow} \cdot \Delta_t + \alpha^{aFRR,\downarrow} \cdot \pi^{aFRR,bal,\downarrow} \cdot R^{aFRR,\downarrow} \cdot \Delta_t}_{\text{activation remuneration}} . \end{aligned} \tag{1}$$

A compact representation of Eq. (1) is given in Eq. (2a), employing upward and downward aFRR composite unitary prices, denoted as $\pi^{aFRR,comp,\uparrow}$ and $\pi^{aFRR,comp,\downarrow}$, respectively. These composite prices, defined in Eq. (2b) for upward aFRR and in Eq. (2c) for downward aFRR, represent the price at which each unit of aFRR capacity is remunerated, considering both availability remuneration and activation remuneration mechanisms.

$$\text{BASMR} = \pi^{FCR} \cdot R^{FCR} + \pi^{aFRR,comp,\uparrow} \cdot R^{aFRR,\uparrow} + \pi^{aFRR,comp,\downarrow} \cdot R^{aFRR,\downarrow}, \tag{2a}$$

$$\pi^{aFRR,comp,\uparrow} = \pi^{aFRR,\uparrow} + \alpha^{aFRR,\uparrow} \cdot \pi^{aFRR,bal,\uparrow} \cdot \Delta_t, \tag{2b}$$

$$\pi^{aFRR,comp,\downarrow} = \pi^{aFRR,\downarrow} + \alpha^{aFRR,\downarrow} \cdot \pi^{aFRR,bal,\downarrow} \cdot \Delta_t. \tag{2c}$$

The aggregator may deviate from the reserve offers. These deficits include the FCR deficit ΔR^{FCR}, upward aFRR deficit $\Delta R^{aFRR,\uparrow}$ (deviation from the original offer of upward aFRR), and downward aFRR deficit $\Delta R^{aFRR,\downarrow}$ (deviation from the original offer of downward aFRR). Similarly to energy imbalances, reserve deficits are penalized by the market operator through market penalties. The FCR deficit penalty price, upward aFRR deficit penalty price and downward aFRR deficit penalty price are denoted by $\pi^{\Delta R,FCR}$, $\pi^{\Delta R,aFRR,\uparrow}$ and $\pi^{\Delta R,aFRR,\downarrow}$, respectively.

Applying the same rationale used to derive Eqs. (2), it is straightforward to derive the cumulative penalty faced by the aggregator in the event of deficits, referred to as the Balancing Ancillary Services Market Penalty (BASMP). This penalty is expressed in Eq. (3a), taking into account

the composite unitary penalty price for upward aFRR deficit, denoted by $\pi^{\Delta R,aFRR,comp,\uparrow}$ and defined in Eq. (3b), and the composite unitary penalty price for downward aFRR deficit, denoted by $\pi^{\Delta R,aFRR,comp,\downarrow}$ and defined in Eq. (3c).

$$\text{BASMP} = \pi^{\Delta R,FCR} \cdot \Delta R^{FCR} + \pi^{\Delta R,aFRR,comp,\uparrow} \cdot \Delta R^{aFRR,\uparrow} + \pi^{\Delta R,aFRR,comp,\downarrow} \cdot \Delta R^{aFRR,\downarrow}, \tag{3a}$$

$$\pi^{\Delta R,aFRR,comp,\uparrow} = \pi^{\Delta R,aFRR,\uparrow} + \alpha^{aFRR,\uparrow} \cdot \pi^{aFRR,bal,\uparrow} \cdot \Delta_t, \tag{3b}$$

$$\pi^{\Delta R,aFRR,comp,\downarrow} = \pi^{\Delta R,aFRR,\downarrow} + \alpha^{aFRR,\downarrow} \cdot \pi^{aFRR,bal,\downarrow} \cdot \Delta_t. \tag{3c}$$

2.2.3. BESS

In the following, a standard state-space model is used to represent the BESS dynamics. The energy stored in the BESS at time t is denoted by x_t, with x^{min} and x^{max} representing the minimum and maximum BESS energy storage levels, respectively. The BESS charging and discharging power are denoted by p^c and p^d, while $p^{c/d,min}$ and $p^{c/d,max}$ represent the minimum and maximum BESS charging/discharging power. The charging and discharging efficiencies are denoted by η_c and η_d respectively.

When operating a BESS, it is necessary to evaluate its degradation as it significantly impacts the cost and performance of the aggregator. In the following, a BESS degradation model based on [43] is proposed. Two types of BESS degradation effects are considered: calendar aging and cycling aging. The former occurs when the BESS is at rest, i.e., there are no current flows through the battery. The latter occurs when the BESS is charged or discharged. Denote by π^B the cost associated to one complete BESS charge/discharge cycle, and by w_{cy} and w_{cl} the weights associated to cycling and calendar aging, respectively. Moreover, denote by $x^{cl,thr}$ the calendar aging threshold (above this level, the BESS is assumed to also be affected by calendar aging). The calendar aging factor $\boldsymbol{cl}(x_t)$ and the cycling aging factor $\boldsymbol{cy}(x_t, x_{t-1})$ are defined in Eq. (4) and Eq. (5), respectively.

$$\boldsymbol{cl}\,(x_t) := w_{cl} \cdot x_t. \tag{4}$$

$$\boldsymbol{cy}\,(x_t, x_{t-1}) := w_{cy} \cdot |x_t - x_{t-1}|\,. \tag{5}$$

The BESS degradation function $\boldsymbol{D}(x_t, x_{t-1})$ is employed to represent BESS aging, as defined in Eq. (6).

$$\boldsymbol{D}\,(x_t, x_{t-1}) := \begin{cases} \pi^B \cdot (\boldsymbol{cl}\,(x_t) + \boldsymbol{cy}\,(x_t, x_{t-1}))\,, & \text{if } x_t \geq x^{cl,thr} \\ \pi^B \cdot \boldsymbol{cy}\,(x_t, x_{t-1})\,, & \text{else} \end{cases}. \tag{6}$$

2.3. Novel two-level stochastic architecture for trading and control

In this section, a novel two-level scenario-based stochastic architecture is presented for the participation of hybrid vRES-BESS systems in the joint energy and balancing AS market. The problem at hand involves the following time stages:

1. **DA step** (24h before energy injection/withdrawal), which corresponds to the **trading problem**, when the aggregator submits energy, FCR and aFRR bids.
2. **ST step** (minutes before energy injection/withdrawal), which corresponds to the **control problem**, when the aggregator updates its schedule in response to the activation of AS.

In the following, the problem is referred to as the **trading and control problem**, and the decision variables and parameters associated with the DA and ST steps are denoted with superscripts DA and ST, respectively.

It is assumed that the energy generated by the vRES power plant, denoted by y, is unknown throughout both stages of the problem, while market prices are considered to be known. The vRES installed capacity is identified as y^{max}. The uncertain parameter y is represented by a specific scenario ω within the set of many scenarios Ω. The uncertain parameters and decision variables associated with the scenario ω are indicated with the subscript ω. Generation of scenarios for the uncertain parameter is achieved through a state-of-the-art approach, specifically the integration of a probabilistic forecast and a Gaussian copula to capture temporal dependencies [42]. Two sets of scenarios of the uncertain parameter realization are considered. First, a set of scenarios Ω^{DA} is generated during the DA step to tackle the trading problem. Second, a new set of scenarios Ω^{ST} is generated during the ST step to tackle the control problem. In addition to vRES energy forecast, the proposed architecture receives as input predicted frequency-control activation signals. Due to the high volatility of these signals in real-time, it is very difficult to obtain a reliable forecast at DA step. In this study, a moving average of the historical data is considered as a forecast for the frequency-control activation signals, denoted with the superscript ˆ, e.g., $\hat{\alpha}^{FCR}$. This forecast is derived by computing the moving average over the last 60 minutes of historical data.

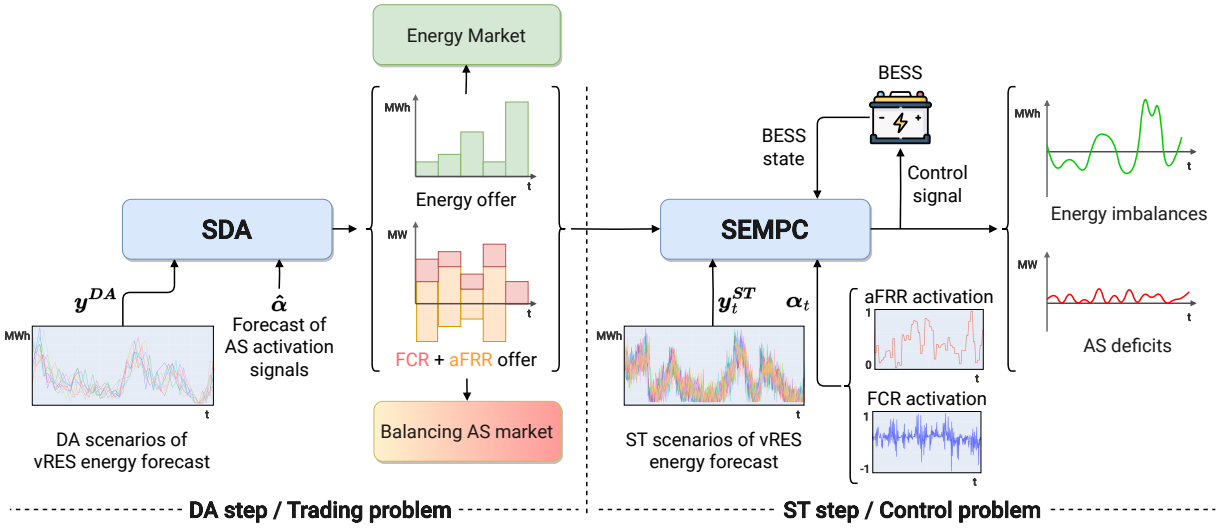

Figure 1: Graphical representation of the proposed SDA+SEMPC architecture to tackle the trading and control problem.

A two-level stochastic architecture is proposed, incorporating optimization-based approaches to address the trading and control problem. First, the stochastic day-ahead (SDA) module employs scenario-based stochastic optimization to tackle the trading problem during the DA step. Second, a scenario-based SEMPC strategy is employed to tackle the control problem during the ST step. This approach is denoted as the **stochastic day-ahead + stochastic economic model predictive control** (**SDA+SEMPC**) architecture. The proposed SDA+SEMPC architecture is shown in Figure 1. During the DA step, the aggregator generates a set of DA vRES energy forecast scenarios

$\boldsymbol{y^{DA}}$ and predictions of the frequency-control AS activation signals $\hat{\boldsymbol{\alpha}}$. Given these inputs, the SDA module computes energy, FCR and aFRR offers for the energy and balancing AS markets. Afterwards, during the ST step, at each time $t \in T$, a new set of ST vRES energy forecast scenarios $\boldsymbol{y_t^{ST}}$ is generated and the aggregator receives the actual frequency-control activation signals $\boldsymbol{\alpha_t}$. Given these inputs, the SEMPC module controls the BESS to optimize the economic objectives of the aggregator (maximize market revenue and minimize storage degradation).

2.3.1. First level: stochastic optimization

The first level of the proposed architecture tackles the trading problem during the DA step. The trading problem is formulated considering a sampling period Δ_t. Given the DA vRES energy forecast as input, this problem consists in deriving a simultaneous offer of energy and AS reserves. The set of DA first-stage decision variables $\boldsymbol{z^{DA,I}}$ and the set of DA second-stage decision variables $\boldsymbol{z^{DA,II}}$ are defined in Eq. (7) and Eq. (8), respectively.

$$\boldsymbol{z^{DA,I}} := \left\{ E_t^{DA}, R_t^{FCR,DA}, R_t^{aFRR,\uparrow,DA}, R_t^{aFRR,\downarrow,DA} \quad \middle| \quad t \in T \right\}. \tag{7}$$

$$\begin{aligned} \boldsymbol{z^{DA,II}} := \Big\{ & \Delta E_{\omega,t}^{\uparrow,DA}, \Delta E_{\omega,t}^{\downarrow,DA}, \Delta R_{\omega,t}^{FCR,DA}, \Delta R_{\omega,t}^{aFRR,\uparrow,DA}, \Delta R_{\omega,t}^{aFRR,\downarrow,DA}, x_{\omega,t}^{DA}, p_{\omega,t}^{c,DA}, p_{\omega,t}^{d,DA}, b_{\omega,t}^{c}, b_{\omega,t}^{d} \quad \Big| \\ & t \in T, \omega \in \Omega^{DA} \Big\}. \end{aligned} \tag{8}$$

To succinctly formulate the problem, it is convenient to introduce the following vectors. The vector of reserve offers is denoted by $\boldsymbol{R_t^{DA}}$ and is defined in Eq. (9).

$$\boldsymbol{R_t^{DA}} := \begin{bmatrix} R_t^{FCR,DA} & R_t^{aFRR,\uparrow,DA} & R_t^{aFRR,\downarrow,DA} \end{bmatrix}^T. \tag{9}$$

The vectors of DA energy imbalances, denoted by $\boldsymbol{\Delta E_{\omega,t}^{DA}}$, DA reserve deficits, denoted by $\boldsymbol{\Delta R_{\omega,t}^{DA}}$, and DA BESS power commands, denoted by $\boldsymbol{P_{\omega,t}^{DA}}$, are defined in Eq. (10), Eq. (11) and Eq. (12), respectively.

$$\boldsymbol{\Delta E_{\omega,t}^{DA}} := \begin{bmatrix} \Delta E_{\omega,t}^{\uparrow,DA} & \Delta E_{\omega,t}^{\downarrow,DA} \end{bmatrix}^T. \tag{10}$$

$$\boldsymbol{\Delta R_{\omega,t}^{DA}} := \begin{bmatrix} \Delta R_{\omega,t}^{FCR,DA} & \Delta R_{\omega,t}^{aFRR,\uparrow,DA} & \Delta R_{\omega,t}^{aFRR,\downarrow,DA} \end{bmatrix}^T. \tag{11}$$

$$\boldsymbol{P_{\omega,t}^{DA}} := \begin{bmatrix} p_{\omega,t}^{c,DA} & p_{\omega,t}^{d,DA} \end{bmatrix}^T. \tag{12}$$

The vectors of reserve prices, denoted by $\boldsymbol{\pi_t^R}$, energy imbalances penalty prices, denoted by $\boldsymbol{\pi_t^{\Delta E}}$, and reserve deficits penalty prices, denoted by $\boldsymbol{\pi_t^{\Delta R}}$, are defined in Eq. (13), Eq. (14), and Eq. (15), respectively.

$$\boldsymbol{\pi_t^R} := \begin{bmatrix} \pi_t^{FCR} & \pi_t^{aFRR,comp,\uparrow} & \pi_t^{aFRR,comp,\downarrow} \end{bmatrix}^T. \tag{13}$$

$$\boldsymbol{\pi_t^{\Delta E}} := \begin{bmatrix} \pi_t^{E,\uparrow} & -\pi_t^{E,\downarrow} \end{bmatrix}^T. \tag{14}$$

$$\boldsymbol{\pi_t^{\Delta R}} := \begin{bmatrix} \pi_t^{\Delta R,FCR} & \pi_t^{\Delta R,aFRR,comp,\uparrow} & \pi_t^{\Delta R,aFRR,comp,\downarrow} \end{bmatrix}^T. \tag{15}$$

The vector of predicted frequency-control activation signals is denoted by $\hat{\boldsymbol{\alpha}}_t$ and is defined in Eq. (16), while the vector of BESS charging and discharging efficiencies is denoted by $\boldsymbol{\eta}$ and is defined in Eq. (17).

$$\hat{\boldsymbol{\alpha}}_t := \begin{bmatrix} \hat{\alpha}_t^{FCR} & \hat{\alpha}_t^{aFRR,\uparrow} & -\hat{\alpha}_t^{aFRR,\downarrow} \end{bmatrix}^T . \tag{16}$$

$$\boldsymbol{\eta} := \begin{bmatrix} \eta_c & -\eta_d \end{bmatrix}^T . \tag{17}$$

During the DA step, the aggregator aims at maximizing market revenue while minimizing storage degradation. Thus, the objective function $\boldsymbol{J^{DA}}$ of the trading problem is composed of three terms, namely energy market revenue, balancing AS market revenue and the BESS degradation function, and is defined in Eq. (18).

$$\begin{aligned} \boldsymbol{J^{DA}} := \frac{1}{|T|\,|\Omega^{DA}|} \sum_{\omega \in \Omega^{DA}} \sum_{t \in T} \Bigg(& \underbrace{-\pi_t^E \cdot E_t^{DA} + \boldsymbol{\pi}_t^{\Delta E^T} \boldsymbol{\Delta E}_{\omega,t}^{\boldsymbol{DA}}}_{\text{energy market revenue}} \underbrace{-\boldsymbol{\pi}_t^{R^T} \boldsymbol{R}_t^{\boldsymbol{DA}} + \boldsymbol{\pi}_t^{\Delta R^T} \boldsymbol{\Delta R}_{\omega,t}^{\boldsymbol{DA}}}_{\text{balancing AS market revenue}} + \\ & + \boldsymbol{D}\left(x_{\omega,t+1}^{DA}, x_{\omega,t}^{DA}\right) \Bigg). \end{aligned} \tag{18}$$

Then, the following **SDA** optimization problem is formulated to address the trading problem during the DA step.

$$\underset{z^{DA,I}, z^{DA,II}}{\operatorname{argmin}} \quad \boldsymbol{J^{DA}} \tag{19a}$$

$$\text{s.t.} \quad E_t^{DA} + \begin{bmatrix} -1 \\ 1 \end{bmatrix}^T \boldsymbol{\Delta E}_{\omega,t}^{\boldsymbol{DA}} + \hat{\boldsymbol{\alpha}}_t{}^T \left(\boldsymbol{R}_t^{\boldsymbol{DA}} - \boldsymbol{\Delta R}_{\omega,t}^{\boldsymbol{DA}} \right) \cdot \Delta_t + \begin{bmatrix} \Delta_t \\ -\Delta_t \end{bmatrix}^T \boldsymbol{P}_{\omega,t}^{\boldsymbol{DA}} = y_{\omega,t}^{DA}, \tag{19b}$$

$$E_t^{DA} + \begin{bmatrix} \Delta_t \\ \Delta_t \\ -\Delta_t \end{bmatrix}^T \boldsymbol{R}_t^{\boldsymbol{DA}} \leq y^{max} \cdot \Delta_t + x^{max}, \tag{19c}$$

$$x_{\omega,t+1}^{DA} = x_{\omega,t}^{DA} + \boldsymbol{\eta}^T \boldsymbol{P}_{\omega,t}^{\boldsymbol{DA}} \cdot \Delta_t, \tag{19d}$$

$$x_{\omega,0}^{DA} = x^i \tag{19e}$$

$$x^{min} \leq x_{\omega,t}^{DA} \leq x^{max}, \tag{19f}$$

$$p^{c,min} \cdot b_{\omega,t}^c \leq p_{\omega,t}^{c,DA} \leq p^{c,max} \cdot b_{\omega,t}^c, \tag{19g}$$

$$p^{d,min} \cdot b_{\omega,t}^d \leq p_{\omega,t}^{d,DA} \leq p^{d,max} \cdot b_{\omega,t}^d, \tag{19h}$$

$$b_{\omega,t}^c + b_{\omega,t}^d \leq 1, \tag{19i}$$

$$b_{\omega,t}^c, b_{\omega,t}^d \in \{0, 1\}, \tag{19j}$$

$$E_t^{DA}, R_t^{FCR,DA} \cdot \Delta_t, R_t^{aFRR,\uparrow/\downarrow,DA} \cdot \Delta_t \in [0, y^{max} \cdot \Delta_t + x^{max}], \tag{19k}$$

$$\Delta E_{\omega,t}^{\uparrow,DA}, \Delta E_{\omega,t}^{\downarrow,DA}, \Delta R_{\omega,t}^{FCR,DA}, \Delta R_{\omega,t}^{aFRR,\uparrow/\downarrow,DA} \in \mathbb{R}_+, \tag{19l}$$

$$\forall \omega \in \Omega^{DA}, \forall t \in T. \tag{19m}$$

Eq. (19b) ensures the energy balance between market offers, energy imbalances, reserve deficits, energy storage and renewable power generation. Eq. (19c) is the market constraint

that imposes offering a total amount of energy lower or equal to the system total capacity. Eqs. (19d)-(19f) describe the BESS dynamics and limits. Eqs. (19g)-(19j) enforce the BESS charging/discharging power limits and avoid simultaneous charging and discharging (by means of the binary variables $b^c_{\omega,t}$ and $b^d_{\omega,t}$). Eqs. (19k)-(19l) define the admissible ranges of the decision variables.

2.3.2. Second level: SEMPC

The second level of the proposed architecture tackles the control problem during the ST step. The control problem is formulated considering a sampling period Δ_k, in general different from the sampling period of the trading problem Δ_t. This problem consists in adapting the aggregator's schedule to answer the activation of frequency-control AS. The second level of the proposed architecture receives as inputs the set of first-stage decisions $\boldsymbol{z^{DA,I}}$ of the trading problem (19), which has been computed during the DA step and is now fixed, and an updated version of vRES energy forecast y^{ST}, namely ST vRES energy forecast. Then, a SEMPC strategy is employed to recompute the second-stage decision variables of the trading problem (19), which will be executed in real-time.

At time t, the SEMPC takes as input the ST scenarios of vRES power generation $y^{ST}_{\omega,t+k}$ and calculates the optimal control sequence $\boldsymbol{u^{ST}}$ for each sampling time k within the prediction horizon K. This sequence encompasses energy imbalances, reserve deficits, and BESS power commands. Subsequently, only the first element $\boldsymbol{u^{ST}_{t|t}}$ of the optimal control sequence is executed at time t, and this process is reiterated in the next time step $t+1$. This methodology adheres to the standard approach in MPC theory, as illustrated, for instance, in [20]. In the following, $\boldsymbol{u^{ST}_{t|t}}$ is kept constant across all scenarios to ensure the feasibility of the control strategy, as shown in [33].

Eq. (20) defines the set of ST decision variables, denoted by $\boldsymbol{z^{ST}}$.

$$\begin{aligned} z^{\boldsymbol{ST}} := \Big\{ & \Delta E^{\uparrow,ST}_{\omega,t+k|t}, \Delta E^{\downarrow,ST}_{\omega,t+k|t}, \Delta R^{FCR,ST}_{\omega,t+k|t}, \Delta R^{aFRR,\uparrow,ST}_{\omega,t+k|t}, \Delta R^{aFRR,\downarrow,ST}_{\omega,t+k|t}, x^{ST}_{\omega,t+k|t}, p^{c,ST}_{\omega,t+k|t}, p^{d,ST}_{\omega,t+k|t}, \\ & b^c_{\omega,t+k|t}, b^d_{\omega,t+k|t} \quad \Big| \quad k \in K, \omega \in \Omega^{ST} \Big\}. \end{aligned} \tag{20}$$

The vectors of ST energy imbalances, denoted by $\boldsymbol{\Delta E^{ST}_{\omega,t+k|t}}$, ST reserve deficits, denoted by $\boldsymbol{\Delta R^{ST}_{\omega,t+k|t}}$, and ST BESS power commands, denoted by $\boldsymbol{P^{ST}_{\omega,t+k|t}}$, are defined in Eq. (21), Eq. (22), and Eq. (23), respectively.

$$\boldsymbol{\Delta E^{ST}_{\omega,t+k|t}} := \begin{bmatrix} \Delta E^{\uparrow,ST}_{\omega,t+k|t} & \Delta E^{\downarrow,ST}_{\omega,t+k|t} \end{bmatrix}^T. \tag{21}$$

$$\boldsymbol{\Delta R^{ST}_{\omega,t+k|t}} := \begin{bmatrix} \Delta R^{FCR,ST}_{\omega,t+k|t} & \Delta R^{aFRR,\uparrow,ST}_{\omega,t+k|t} & \Delta R^{aFRR,\downarrow,ST}_{\omega,t+k|t} \end{bmatrix}^T. \tag{22}$$

$$\boldsymbol{P^{ST}_{\omega,t+k|t}} := \begin{bmatrix} p^{c,ST}_{\omega,t+k|t} & p^{d,ST}_{\omega,t+k|t} \end{bmatrix}^T. \tag{23}$$

During the ST step, the aggregator aims to minimize market penalties and storage degradation, while answering the activation of frequency-control AS. Thus, the objective function $\boldsymbol{J^{ST}}$ of the control problem is composed of three terms, namely energy market penalties, balancing AS market

penalties and the BESS degradation function, and is defined in Eq. (24).

$$\boldsymbol{J^{ST}} = \frac{1}{|K|\,|\Omega^{ST}|} \sum_{\omega\in\Omega^{ST}} \sum_{k\in K} \Bigg(\underbrace{\boldsymbol{\pi}_{t+k}^{\boldsymbol{\Delta E}^T}\, \boldsymbol{\Delta E}_{\omega,t+k|t}^{\boldsymbol{ST}}}_{\text{energy market penalties}} + \underbrace{\boldsymbol{\pi}_{t+k}^{\boldsymbol{\Delta R}^T}\, \boldsymbol{\Delta R}_{\omega,t+k|t}^{\boldsymbol{ST}}}_{\text{balancing AS market penalties}} + \boldsymbol{D}\left(x_{\omega,t+k+1|t}^{ST}, x_{\omega,t+k|t}^{ST}\right) \Bigg). \quad (24)$$

Then, the following **SEMPC** strategy is formulated to address the control problem during the ST step.

$$\underset{\boldsymbol{u}_{t|t}^{\boldsymbol{ST}}, \boldsymbol{z}^{\boldsymbol{ST}}}{\operatorname{argmin}} \quad \boldsymbol{J^{ST}} \quad (25a)$$

$$\text{s.t.} \quad E_{t+k}^{DA} + \begin{bmatrix} -1 \\ 1 \end{bmatrix}^T \boldsymbol{\Delta E}_{\omega,t+k|t}^{\boldsymbol{ST}} + \boldsymbol{\alpha}_t{}^T \left(\boldsymbol{R}_{t+k}^{\boldsymbol{DA}} - \boldsymbol{\Delta R}_{\omega,t+k|t}^{\boldsymbol{ST}} \right) \cdot \Delta_k + \begin{bmatrix} \Delta_k \\ -\Delta_k \end{bmatrix}^T \boldsymbol{P}_{\omega,t+k|t}^{\boldsymbol{ST}} = y_{\omega,t+k}^{ST}, \quad (25b)$$

$$\left[\boldsymbol{\Delta E}_{\omega,t|t}^{\boldsymbol{ST}\ T} \quad \boldsymbol{\Delta R}_{\omega,t|t}^{\boldsymbol{ST}\ T} \quad \boldsymbol{P}_{\omega,t|t}^{\boldsymbol{ST}\ T} \right]^T = \boldsymbol{u}_{t|t}^{\boldsymbol{ST}}, \quad (25c)$$

$$x_{\omega,t+k+1|t}^{ST} = x_{\omega,t+k|t}^{ST} + \boldsymbol{\eta}^T \boldsymbol{P}_{\omega,t+k|t}^{\boldsymbol{ST}} \cdot \Delta_k, \quad (25d)$$

$$x_{\omega,t|t}^{ST} = x_0 \quad (25e)$$

$$x^{min} \le x_{\omega,t+k|t}^{ST} \le x^{max}, \quad (25f)$$

$$p^{c,min} \cdot b_{\omega,t+k|t}^{c} \le p_{\omega,t+k|t}^{c,ST} \le p^{c,max} \cdot b_{\omega,t+k|t}^{c}, \quad (25g)$$

$$p^{d,min} \cdot b_{\omega,t+k|t}^{d} \le p_{\omega,t+k|t}^{d,ST} \le p^{d,max} \cdot b_{\omega,t+k|t}^{d}, \quad (25h)$$

$$b_{\omega,t+k|t}^{c} + b_{\omega,t+k|t}^{d} \le 1, \quad (25i)$$

$$b_{\omega,t+k|t}^{c}, b_{\omega,t+k|t}^{d} \in \{0,1\}, \quad (25j)$$

$$\boldsymbol{\Delta R}_{\omega,t+k|t}^{\boldsymbol{ST}} \le \boldsymbol{R}_{t+k}^{\boldsymbol{DA}}, \quad (25k)$$

$$\Delta E_{\omega,t+k|t}^{\uparrow,ST}, \Delta E_{\omega,t+k|t}^{\downarrow,ST}, \Delta R_{\omega,t+k|t}^{FCR,ST}, \Delta R_{\omega,t+k|t}^{aFRR,\uparrow,ST}, \Delta R_{\omega,t+k|t}^{aFRR,\downarrow,ST} \in \mathbb{R}_+, \quad (25l)$$

$$\forall \omega \in \Omega^{ST}, \forall k \in K. \quad (25m)$$

Eq. (25b) ensures the energy balance between market offers, energy imbalances, reserve deficits, energy storage and renewable power generation. Eq. (25c) is introduced to force the control strategy to be equal across all scenarios in the first prediction step of the MPC strategy, as shown in [33]. Eqs. (25d)-(25f) describe the BESS dynamics and limits. Eqs. (25g)-(25j) enforce the BESS charging/discharging power limits and avoid simultaneous charging and discharging (by means of the binary variables $b_{\omega,t+k|t}^{c}$ and $b_{\omega,t+k|t}^{d}$). Eqs. (25k)-(25l) define the admissible ranges of the decision variables.

Finally, the two levels involved in our sequential SDA+SEMPC architecture are implemented as shown in Algorithm 1.

2.4. Benchmark approaches for trading and control

To assess the benefits of the novel SDA+SEMPC architecture, two standard MPC-based architectures employing deterministic models are presented in the following. The first benchmark approach employs deterministic optimization to tackle the trading problem and a RTMPC strategy

Algorithm 1: SDA+SEMPC architecture

Data: $\boldsymbol{d} = \left\{x^i, x^{min}, x^{max}, p^{c,min}, p^{d,min}, p^{c,max}, p^{d,max}, \eta_c, \eta_d, y^{max}\right\}$.
First level:
Generate DA vRES energy forecast scenarios $\boldsymbol{y^{DA}} = \left\{y^{DA}_{\omega,t} \quad | \quad \omega \in \Omega^{DA}, t \in T\right\}$;
Generate predicted frequency-control activation signals $\hat{\boldsymbol{\alpha}}$;
$\boldsymbol{z^{DA,I\star}}, \boldsymbol{z^{DA,II\star}} \leftarrow \text{SDA}\left(\boldsymbol{d}, \boldsymbol{y^{DA}}, \hat{\boldsymbol{\alpha}}\right)$;
Second level:
$x_0 \leftarrow x^i$;
$t \leftarrow 0$;
while $t \leq |T| - |K|$ **do**
  Generate ST vRES energy forecast scenarios $\boldsymbol{y_t^{ST}} = \left\{y^{ST}_{\omega,t+k} \quad | \quad \omega \in \Omega^{ST}, k \in K\right\}$;
  Receive the frequency-control activation signals $\boldsymbol{\alpha}_t$ from the TSO ;
  $\boldsymbol{z_t^{DA,I\star}} = \left\{z_{t+k} \in \boldsymbol{z^{DA,I\star}} \quad | \quad k \in K\right\}$;
  $\boldsymbol{u^{ST\star}_{t|t}}, \boldsymbol{z^{ST\star}} \leftarrow \text{SEMPC}\left(\boldsymbol{d}, x_0, \boldsymbol{y_t^{ST}}, \boldsymbol{\alpha}_t, \boldsymbol{z_t^{DA,I\star}}\right)$;
  Apply $\boldsymbol{u^{ST\star}_{t|t}}$;
  $x_0 \leftarrow x_{t+1}$;
  $t \leftarrow t + 1$;
end

to tackle the control problem. This is called the **deterministic day-ahead + deterministic reference tracking model predictive control** (**DDA+DRTMPC**) architecture. The second benchmark approach employs deterministic optimization to tackle the trading problem and an EMPC strategy to tackle the control problem. This is called the **deterministic day-ahead + deterministic economic model predictive control** (**DDA+DEMPC**) architecture.

Our SDA+SEMPC shows two main differences compared to the proposed benchmark approaches:

- **SDA+SEMPC employs economic-oriented control**, while the DDA+DRTMPC employs the traditional reference-tracking strategy to tackle the ST step/control problem.
- **SDA+SEMPC employs a stochastic model** to handle the uncertainty, while both of benchmark strategies employ a deterministic model.

Table 2 summarizes the main differences between DDA+DRTMPC, DDA+DEMPC and our SDA+SEMPC.

Since these benchmark strategies employ deterministic models, the uncertain parameter y is now modeled by a single scenario. Therefore, in the following, the subscript ω is dropped.

2.4.1. First benchmark approach: DDA+DRTMPC

Similar to the proposed SDA+SEMPC architecture, the DDA+DRTMPC consists of two distinct levels. The first level is formulated as (19), where now the set of DA vRES energy forecast

Architecture	Economic-oriented predictive control	Stochastic model
DDA+DRTMPC	-	-
DDA+DEMPC	✓	-
SDA+SEMPC	✓	✓

Table 2: Comparison between our SDA+SEMPC and the proposed benchmark approaches.

scenarios is reduced to a single scenario, i.e., $|\Omega^{DA}| = 1$. The second level employs a traditional RTMPC approach to tackle the control problem during the ST step.

Unlike the objective function of our SEMPC, the control strategy of the RTMPC is designed to minimize the squared difference between the BESS schedule computed during the DA step and that of the ST step. This tracking error is defined in Eq. (26).

$$\boldsymbol{eb}^{\mathbf{2}}_{t+k|t} := \left(x^{DA}_{t+k} - x^{ST}_{t+k|t}\right)^2 . \tag{26}$$

Moreover, the quadratic terms defined in Eq. (27) and Eq. (28) are introduced to penalize the energy imbalances and the reserve deficits, respectively.

$$\boldsymbol{\delta E}^{\mathbf{2}}_{t+k|t} := \left(\Delta E^{\uparrow,ST}_{t+k|t}\right)^2 + \left(\Delta E^{\downarrow,ST}_{t+k|t}\right)^2 . \tag{27}$$

$$\boldsymbol{\delta R}^{\mathbf{2}}_{t+k|t} := \left(\Delta R^{FCR,ST}_{t+k|t}\right)^2 + \left(\Delta R^{aFRR,\uparrow,ST}_{t+k|t}\right)^2 + \left(\Delta R^{aFRR,\downarrow,ST}_{t+k|t}\right)^2 . \tag{28}$$

Then, the optimization problem solved by the RTMPC to tackle the control problem during the ST step is formulated as

$$\underset{z^{ST}}{\text{argmin}} \quad \sum_{k\in K} \left(\boldsymbol{eb}^{\mathbf{2}}_{t+k|t} + \boldsymbol{\delta E}^{\mathbf{2}}_{t+k|t} + \boldsymbol{\delta R}^{\mathbf{2}}_{t+k|t}\right) \tag{29a}$$

$$\text{s.t.} \quad (25b), (25d) - (25l), \tag{29b}$$

$$\forall k \in K, \tag{29c}$$

where the decision variables in $\boldsymbol{z^{ST}}$ and the constraints (29b) are reduced to the case of a single scenario of the uncertain parameter realization, i.e., $|\Omega^{ST}| = 1$.

2.4.2. Second benchmark approach: DDA+DEMPC

Similarly to our approach, the DDA+DEMPC architecture is composed of two levels. The first level is formulated in the same way as in the DDA+RTMPC architecture. The second level employs an EMPC strategy to tackle the control problem. In this case, the control strategy is aware of market prices, as in our SEMPC, but it employs a deterministic model to handle the uncertainty, as in the RTMPC.

Thus, the optimization problem solved by the EMPC to tackle the control problem during the ST step is formulated as

$$\underset{z^{ST}}{\text{argmin}} \quad \boldsymbol{J^{ST}} \tag{30a}$$

$$\text{s.t.} \quad (29b) \tag{30b}$$

$$\forall k \in K, \tag{30c}$$

where the decision variables in $\boldsymbol{z^{ST}}$ and the objective function $\boldsymbol{J^{ST}}$ are reduced to the case of a single scenario of the uncertain parameter realization, i.e., $|\Omega^{ST}| = 1$.

3. Case study description

A real hybrid power plant, consisting of an onshore wind farm and a stationary BESS operating under the same grid connection point, is examined. Historical time-series of wind power production are considered, sourced from the Smart4RES EU Project [38]. A simulation period of three months is considered (from August to October 2020). To ensure confidentiality, the capacities of the hybrid system components are scaled by the installed capacity y^{max} of the wind farm. Thus, the capacity of the BESS is 0.2MW/0.2MWh for a 1MW wind farm capacity. The parameters of the BESS degradation model (6) are derived following the energy throughput degradation model proposed in [43]. The parameter values used to perform the following simulations are reported in Table 3.

Parameter	Symbol	Value
vRES installed capacity	y^{max}	1 MW
BESS energy range	$\left[x^{min}, x^{max}\right]$	[0.04, 0.2] MWh
BESS charging/discharging power range	$\left[p^{c/d,min}, p^{c/d,max}\right]$	[0, 0.2] MW
BESS initial state	x^{i}	$0.5 \cdot x^{max}$
Calendar aging threshold	$x^{cl,thr}$	$0.8 \cdot x^{max}$
BESS charging efficiency	η_c	0.95
BESS discharging efficiency	η_d	$\frac{1}{0.95}$
Cost of a complete BESS charge/discharge cycle	π^{B}	20 RON/MWh
BESS cycling aging weight	w_{cy}	0.79
BESS calendar aging weight	w_{cl}	2.75
DA step/Trading problem sampling period	Δ_t	1h
ST step/Control problem sampling period	Δ_k	5min

Table 3: Simulation parameters.

Both Ω^{DA} and Ω^{ST} include 10 scenarios of the uncertain parameter realization. The former set comprises scenarios at a 1-hour resolution, while the latter includes scenarios at a 5-minute resolution. The SDA+SEMPC utilizes these sets of scenarios, whereas the deterministic benchmarks use a vRES forecast profile obtained by averaging over the set of vRES forecast scenarios. Figure 2 characterizes the vRES forecast and its absolute error.

As described in section 2.2.2, the activation of balancing energy is driven by activation signals sent by the TSO to the BSP. Figure 3 shows the observed average daily FCR and aFRR activation signals, namely α^{FCR}, $\alpha^{aFRR,\uparrow}$ and $\alpha^{aFRR,\downarrow}$.

Reference is made to the Romanian energy and balancing AS markets; consequently, all prices are expressed in the Romanian currency (RON). To conduct the simulations outlined in the following section, we consider historical time-series of hourly prices for energy and balancing AS

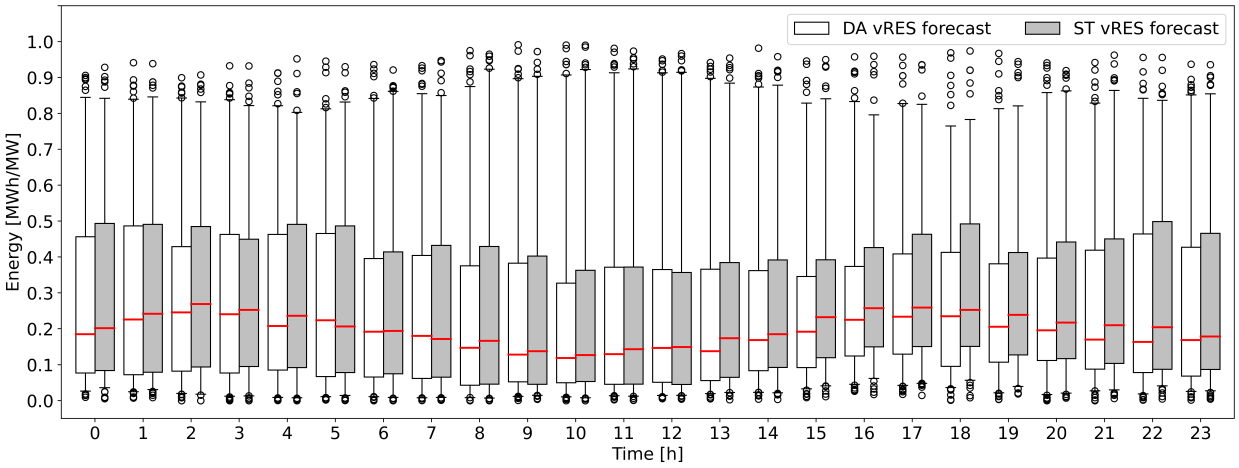

(a) DA and ST vRES forecasts as a function of the hour of the day.

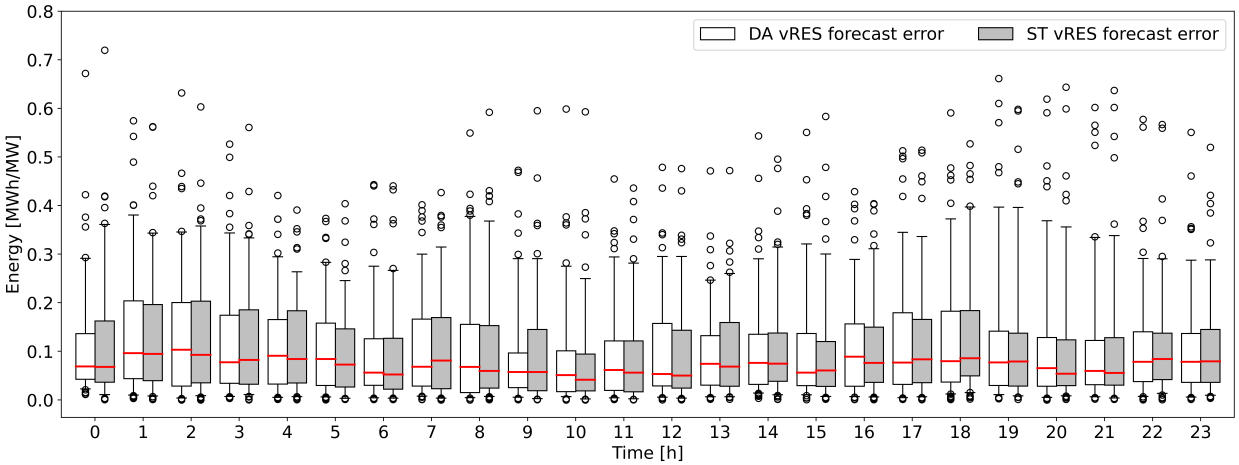

(b) Absolute error of DA and ST vRES forecasts as a function of the hour of the day.

Figure 2: Boxplots of the vRES forecast and the absolute error of vRES forecast (absolute value of the difference between real and forecast generation) as a function of the hour of the day. Both plots encapsulate data from the entire three-month simulation period. The box represents the interquartile range, the line in the box is the median, and the whiskers are set at the 5 and 95 percentile of the data range. Values are in MWh/MW since vRES energy is normalized by the nominal capacity of the hybrid system.

during the three-month simulation period. Table 4 reports the observed average prices, offering a characterization of the markets under consideration.

Simulations were carried out on a personal computer equipped with an Intel(R) Core(TM) i7-10850H processor and 16GB of RAM. Python 3.8 was utilized as the programming language for implementation, and Gurobi served as the solver. The computational performance of the SEMPC and the proposed benchmarks is documented in Table 5.

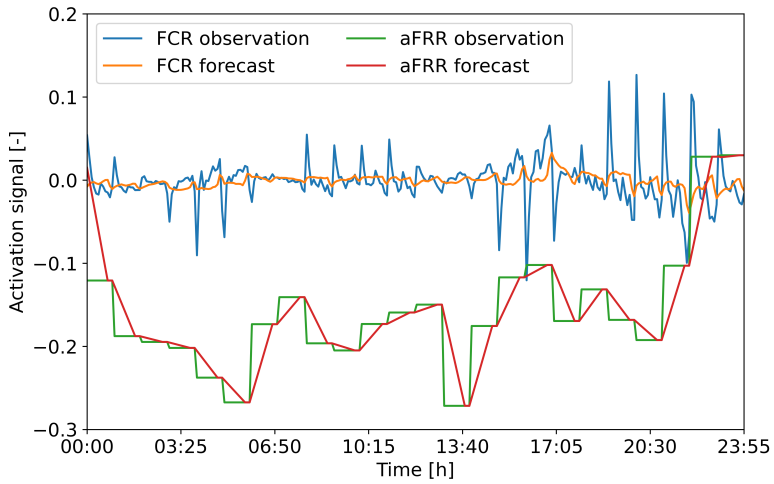

Figure 3: Average hourly forecast and observation of FCR activation signal (α^{FCR}), and average hourly forecast and observation of net aFRR activation signal (difference between $\alpha^{aFRR,\uparrow}$ and $\alpha^{aFRR,\downarrow}$). The forecast of AS activation signals is determined by calculating the moving average over the preceding 60 minutes of historical data. The figure illustrates the average values calculated for each hour of the day, considering the entirety of the three-month simulation period.

Parameter	**Symbol**	**Value**
Energy market		
Energy price	π^{E}	203.7 RON/MWh/h
Penalty price of negative energy imbalance	$\pi^{E,\uparrow}$	615 RON/MWh/h
Penalty price of positive energy imbalance	$\pi^{E,\downarrow}$	-8.5 RON/MWh/h
Balancing AS market		
FCR price	π^{FCR}	204 RON/MW/h
Penalty price of FCR deficit	$\pi^{\Delta R,FCR}$	1019 RON/MW/h
Upward/Downward aFRR price	$\pi^{aFRR,\uparrow/\downarrow}$	65.5 RON/MW/h
Penalty price of upward/downward aFRR deficit	$\pi^{\Delta R,aFRR,\uparrow/\downarrow}$	327.3 RON/MW/h
Price of activated upward aFRR balancing energy	$\pi^{aFRR,bal,\uparrow}$	691.8 RON/MWh/h
Price of activated downward aFRR balancing energy	$\pi^{aFRR,bal,\downarrow}$	27.7 RON/MWh/h

Table 4: Average prices of the Romanian energy and balancing AS markets.

Strategy	**MPC iteration time [s]**
DRTMPC	1 (0.4)
DEMPC	1 (0.3)
SEMPC	**4.3 (1.7)**

Table 5: Computational performance. Mean value and standard deviation (in brackets).

4. Results

In the following, a comparison is proposed between our novel scenario-based fully stochastic architecture for trading and control, namely the SDA+SEMPC architecture, and the deterministic

benchmark approaches detailed in sections 2.4.1 and 2.4.2, referred to as DDA+DRTMPC and DDA+DEMPC, respectively. First, the observed ex-post market revenue and BESS degradation are presented in two different cases: one where the aggregator participates solely in the energy market and another where participation occurs in both the energy and balancing AS market. Second, an investigation into the performance of the economic-oriented control strategy is conducted, contrasting it with the traditional non-economic-oriented reference-tracking control. Finally, it is shown that the utilization of a stochastic model to handle uncertainty significantly enhances the reliability of the decision framework, compared to the proposed benchmark strategies.

4.1. Ex-post evaluation

Table 6 shows a comparison between our SDA+SEMPC and the proposed benchmarks in terms of the observed ex-post market revenue and BESS degradation, when the aggregator is assumed to participate only in the energy market. As expected, the economic-oriented architec-

Strategy	Market Revenue [RON/MW/h]	BESS Degradation [RON/MW/h]
DDA + DRTMPC	24.6 (70)	0.62 (1.6)
DDA + DEMPC	24.8 (69.9)	0.5 (1.3)
SDA + SEMPC	**26.3 (66.8)**	**0.52 (1)**

Table 6: Normalized revenue and BESS degradation when participating only in the energy market. Hourly mean value and standard deviation (in brackets). Values are in RON/MW/h since the energy generation is normalized by both the nominal capacity of the hybrid system and the number of hours in the simulation period.

tures (DDA+DEMPC and SDA+SEMPC) are able to outperform the traditional DDA+DRTMPC. Indeed, once the trading decisions are fixed at the end of the DA step, the economic-oriented architectures employ the knowledge of market prices to directly optimize the economic objectives of the problem at ST, while the traditional non-economic DDA+DRTMPC simply tracks the DA decisions, which may results to be not optimal due to vRES energy forecast errors. Compared to the DDA+DEMPC architecture, our SDA+SEMPC achieves a 7% increase in the revenue at the price of a 4% increase in the storage degradation. Moreover, the SDA+SEMPC significantly reduces the standard deviation of both objectives, compared to the proposed benchmarks. This shows the superior ability of our fully stochastic approach to hedge against the effect of uncertain renewable power generation, compared to benchmark strategies employing deterministic models to handle the uncertainty.

Table 7 shows a comparison between our SDA+SEMPC and the proposed benchmarks, when participating in the joint energy and balancing AS market. Similarly to the energy only case, the economic-oriented approaches (DDA+DEMPC and SDA+SEMPC) significantly outperform the traditional DDA+DRTMPC approach. Our SDA+SEMPC shows a 15% increase in revenue and a 23% decrease in BESS degradation, compared to the traditional DDA+DRTMPC, as well as a reduction in the standard deviation. This again confirms the reliability improvement achieved by our fully stochastic architecture compared to the deterministic benchmarks.

To assess the impact of all sources of uncertainty, consideration is given to the case of unknown market prices (persistent prices) and the ideal scenario of known prices and known AS activation signals (perfect prices, perfect AS activation) when employing the DDA+DEMPC benchmark.

Strategy	Market Revenue [RON/MW/h]	BESS Degradation [RON/MW/h]
Market modeling: Perfect prices, Persistent AS activation		
DDA+DRTMPC	264.8 (99.35)	1.3 (1.4)
DDA+DEMPC	301.43 (86.27)	0.97 (1.4)
SDA+SEMPC	**303.76 (83.4)**	**1 (1.2)**
Market modeling: Persistent prices, Persistent AS activation		
DDA+DEMPC	222.4 (169.6)	1 (1.4)
Market modeling: Perfect prices, Perfect AS activation		
DDA+DEMPC	301.49 (86.15)	1 (1.4)

Table 7: Normalized revenue and BESS degradation when participating in the energy and balancing AS markets. Hourly mean value and standard deviation (in brackets). Values are in RON/MW/h since the energy generation is normalized by both the nominal capacity of the hybrid system and the number of hours in the simulation period.

In the former case, a significant reduction in the ex-post market revenue is observed, showing that price uncertainty can significantly impact the performances of the decision framework. Conversely, in the latter case, adding a perfect knowledge of AS activation results in a minor increase in the market revenue, compared to considering persistent AS activation. In both cases, the ex-post storage degradation is almost unchanged.

To conclude this analysis, Table 8 presents the ex-post energy imbalances and reserve deficits. On average, both economic-oriented approaches manage to avoid reserve deficits, indicating higher reliability in providing AS compared to the DDA+DRTMPC benchmark. To

Strategy	Imbalances [MWh/MW/h]		Deficits [MWh/MW/h]		
	$\Delta E^{\uparrow}$	$\Delta E^{\downarrow}$	$\Delta R^{FCR}\Delta_t$	$\Delta R^{aFRR,\uparrow}\Delta_t$	$\Delta R^{aFRR,\downarrow}\Delta_t$
DDA + DRTMPC	0.04 (0.1)	0.43 (0.39)	0.003 (0.01)	0.03 (0.08)	0.12 (0.15)
DDA + DEMPC	0.04 (0.11)	0.48 (0.44)	0 (0)	0 (0)	0 (0)
SDA + SEMPC	**0.04 (0.1)**	**0.5 (0.44)**	**0 (0)**	**0 (0)**	**0 (0)**

Table 8: Normalized energy imbalances, FCR deficit and aFRR deficits, when participating in the energy and balancing AS markets. Hourly mean value and standard deviation (in brackets). Values are in MWh/MW/h since imbalances and deficits are normalized by both the nominal capacity of the hybrid system and the number of hours in the simulation period.

achieve this without significantly increasing the storage degradation, both the DDA+DEMPC and SDA+SEMPC architectures experience, on average, larger deviations from the energy offer compared to those of DDA+DRTMPC. This is motivated by the observed market prices, which penalize reserve deficits significantly more than the energy imbalances (see Table 4). High penalty prices are expected to have a small impact on the traditional DDA+DRTMPC approach, whose control strategy is insensitive to prices, and a significant impact on the economic-oriented approaches, whose control strategy is driven by market prices. Indeed, a traditional reference-tracking approach will tend to distribute the deviations among all services, while an economic-oriented strategy will tend to concentrate them on the less profitable markets only. Thus, under the observed price conditions, when choosing DDA+DEMPC or SDA+SEMPC instead of

DDA+DRTMPC, a reduction in the revenue obtained from the energy market is expected, in exchange for an increase in the revenue obtained from the balancing AS market and a decrease in storage degradation.

4.2. Economic-oriented control versus reference-tracking control

In the following, a comparison is made between the economic-oriented control strategy of the SDA+SEMPC and a traditional reference-tracking control approach, whose control strategy is insensitive to prices. In Figure 4, a comparison is made between the typical BESS state of charge (SoC) daily variation of the SDA+SEMPC approach and that of the DDA+DRTMPC benchmark. During this day, there is no activation of FCR and aFRR prices are constant. Thus, the storage

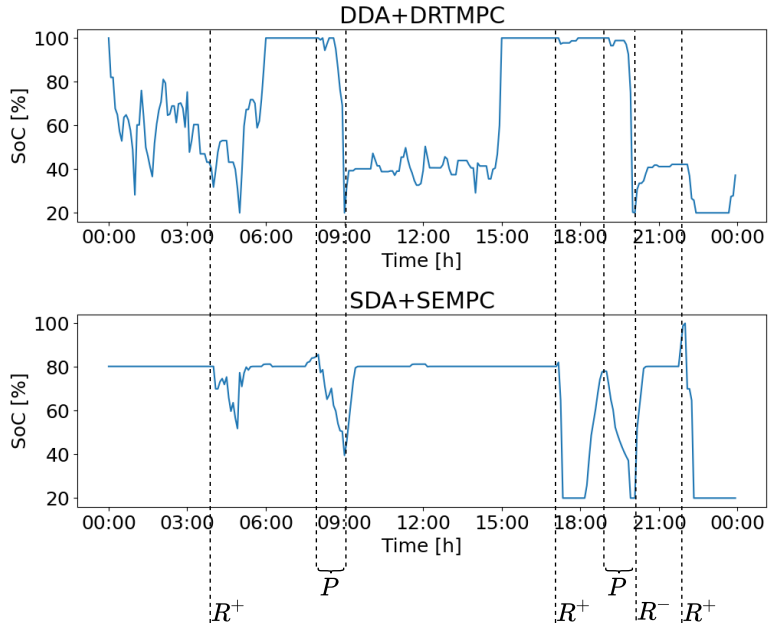

Figure 4: Typical daily variation in the BESS SoC with DDA+DRTMPC (top) and SDA+SEMPC (bottom). P identifies energy peak price periods, while R^+ and R^- identify activation of upward and downward aFRR balancing energy, respectively.

commands are mostly driven by energy prices and aFRR activation signals. The evolution of the storage SoC can be linked to three main events: periods of *energy peak prices*, denoted by P, and the *activation times of upward and downward aFRR balancing energy*, denoted by R^+ and R^-, respectively. Two energy peak price periods occur, first in the morning, then in the late evening. Since prices are assumed to be known already during the DA step, both strategies are able to identify these events and discharge the storage to capitalize on this favorable market condition. On the contrary, when aFRR is activated, the DDA+DRTMPC architecture is not always able to respond appropriately. This is a consequence of the fact that the DDA+DRTMPC strategy aims to track the BESS scheduling computed at DA, that may not coincide with the optimal economic schedule of the ST step. Thus, when a first R^+ period occurs (approximately at 4 a.m.) the DDA+DRTMPC charges the BESS to follow the DA schedule, instead of discharging it to maximize the profit.

When a second activation of upward aFRR occurs (approximately at 5 p.m.) our SDA+SEMPC fully discharges the BESS, while the DDA+DRTMPC shows only a very small discharge, resulting in a large reserve deficit. Moreover, at R^{-} (approximately at 8 p.m.), when the storage is expected to charge to compensate for a downward aFRR activation, the traditional strategy shows only a minor charge, since again the tracked DA BESS schedule is unable to identify this major event. Finally, Figure 4 clearly shows the drawbacks arising from not including the BESS degradation model in the control strategy. Indeed, compared to our SDA+SEMPC, the DDA+DRTMPC benchmark shows many more smaller charge/discharge cycles, resulting in higher cycling aging, and it is kept above $x^{cl,thr}$ for long periods, resulting in higher calendar aging as well.

For a more comprehensive understanding of the advantages of an economically oriented control, Figure 5 illustrates an example of BESS SoC variations with SDA+SEMPC when delivering both energy and FCR. Throughout this timeframe, the hybrid system abstains from contributing to aFRR. When the energy price is higher than the FCR price (at 10 a.m. and 11 a.m.), the aggregator exclusively offers energy. Conversely, when the FCR price exceeds the energy price, the aggregator solely engages in providing FCR. At both 11 a.m. and 12 a.m., unforeseen deficiencies in vRES generation occur. As the BESS lacks sufficient capacity to cover shortages in both hours, a decision is required on how to distribute deviations between the two markets. Given that the proposed controller incorporates knowledge of market prices, the BESS is operated to minimize the FCR deficit at 12 a.m., even at the expense of incurring penalties for an energy imbalance (at 11 a.m.). In contrast, a conventional reference-tracking control strategy would evenly distribute deviations between the two markets, resulting in a less profitable solution compared to that of the SDA+SEMPC, as confirmed by the results shown in Table 7.

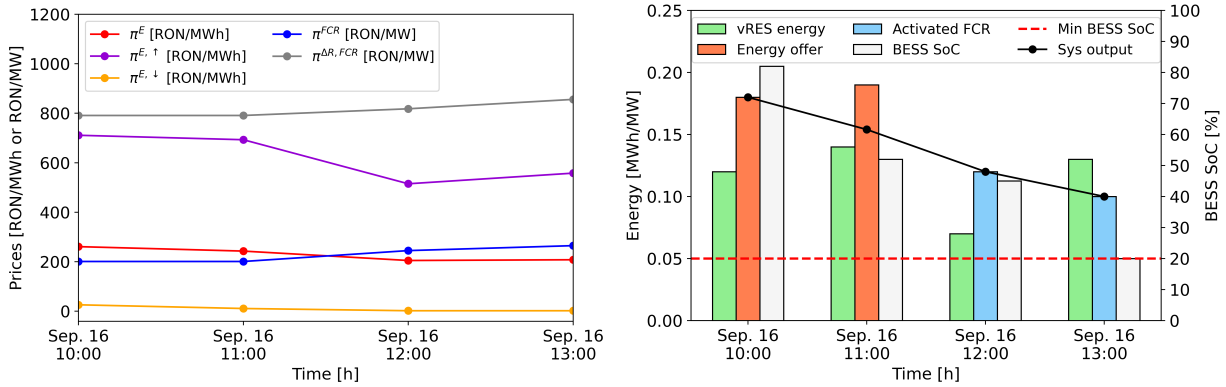

(a) Hourly prices of energy market and balancing AS market.

(b) BESS SoC, offers, vRES energy and hybrid system output.

Figure 5: Example of BESS SoC variations with SDA+SEMPC when providing energy and FCR. For each hour, the figure provides market prices, the initial BESS SoC, the energy offer, activated FCR balancing energy, and the total output of the hybrid system. Energy values are normalized by the nominal capacity of the hybrid system.

4.3. Stochastic model versus deterministic model

As shown in Table 7, both of the DDA+DEMPC and SDA+SEMPC show similar ex-post results. Nevertheless, our stochastic approach improves reliability when forecast errors occur.

In Figure 6, an example is presented wherein our SDA+SEMPC is shown to be more reliable than the DDA+DEMPC benchmark. As depicted in Figure 6a, utilizing a stochastic model in the SDA+SEMPC leads to a more conservative energy offer compared to that of the DDA+DEMPC. In real-time, the aggregator faces a critical period (red area in Figure 6) in which the vRES power generation is significantly lower than what was predicted at DA (see Figure 6b). In this critical period, our SDA+SEMPC shows a superior ability to hedge against the effect of uncertainty, compared to DDA+DEMPC. Indeed, while the conservative behavior of our SDA+SEMPC results in a small energy imbalance, the aggressive bidding strategy of DDA+DEMPC results in a much more imbalanced position (see Figure 6c). This in turns results in a large drop in the ex-post market revenue obtained via DDA+DEMPC, compared to almost no effect observed when our SDA+SEMPC is employed (see Figure 6d).

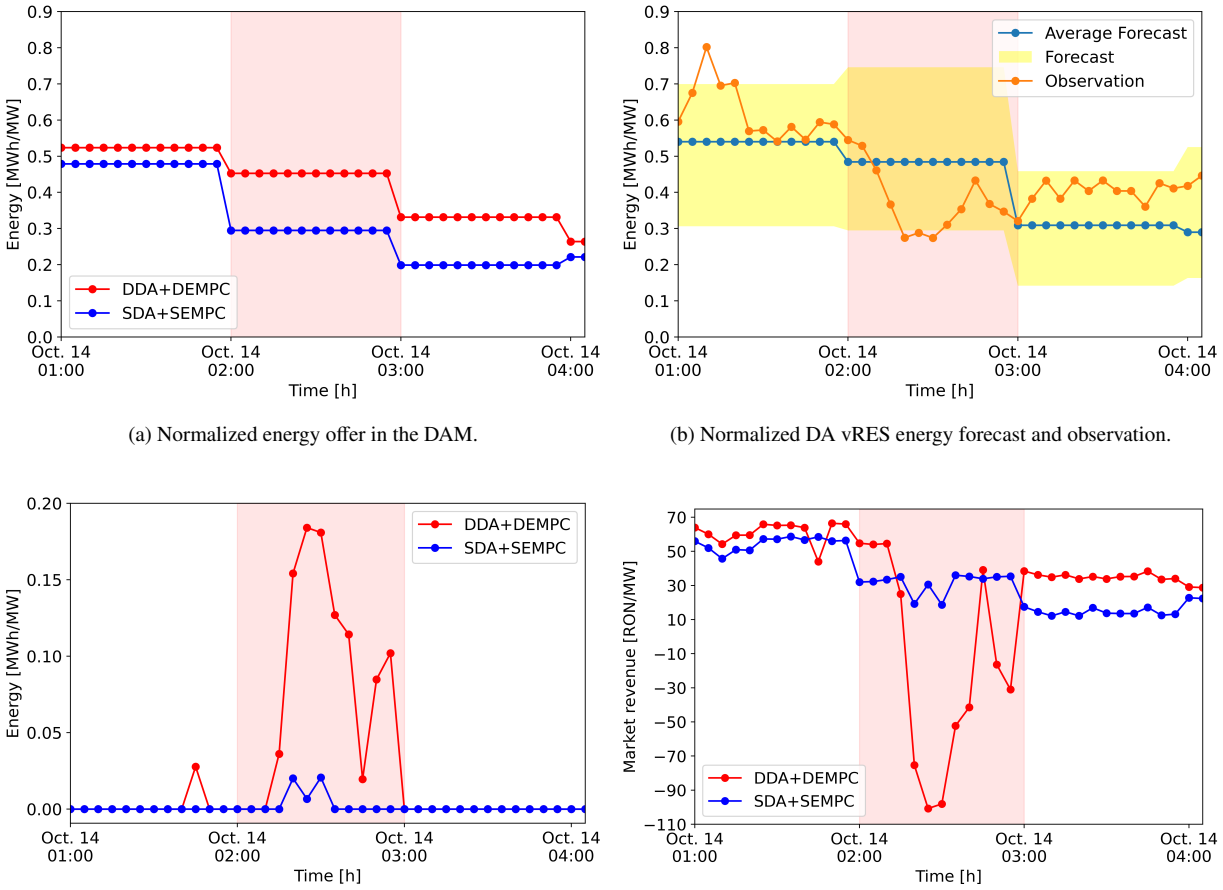

(a) Normalized energy offer in the DAM.

(b) Normalized DA vRES energy forecast and observation.

(c) Normalized ex-post energy imbalance.

(d) Normalized ex-post market revenue.

Figure 6: Normalized energy offer in the DAM, ex-post energy imbalance and ex-post revenue of our SDA+SEMPC, compared to those of the DDA+DEMPC benchmark, when significant DA vRES energy forecast errors occur. Values are normalized by the nominal capacity of the hybrid system.

To generalize the conclusions drawn from the previous example, an analysis is conducted on the impact of vRES energy forecast errors on the observed ex-post DA objective function value, i.e., the value of $\boldsymbol{J}^{DA}$ once the uncertainty is realized. Define the ST vRES energy forecast

error at time t as the difference between the mean ST vRES energy forecast $y^{ST}_{t,\omega}$ and the observed realization of the uncertainty y_t, i.e., $y_t - \frac{1}{|\Omega^{ST}|}\sum_{\omega\in\Omega^{ST}} y^{ST}_{t,\omega}$.

Figure 7 shows the mean and standard deviation of the normalized ex-post DA objective function values obtained with SDA+SEMPC and DDA+DEMPC, as a function of the ST vRES energy forecast error. Our SDA+SEMPC lowers both the mean and standard deviation of $\boldsymbol{J}^{\boldsymbol{DA}}$ compared to DDA+DEMPC, achieving up to 9% decrease in the mean value and up to 13% decrease in the standard deviation. Thus, our SDA+SEMPC is shown to significantly reduce the sensitivity to vRES energy forecast errors, compared to a decision framework employing deterministic models to handle the uncertainty.

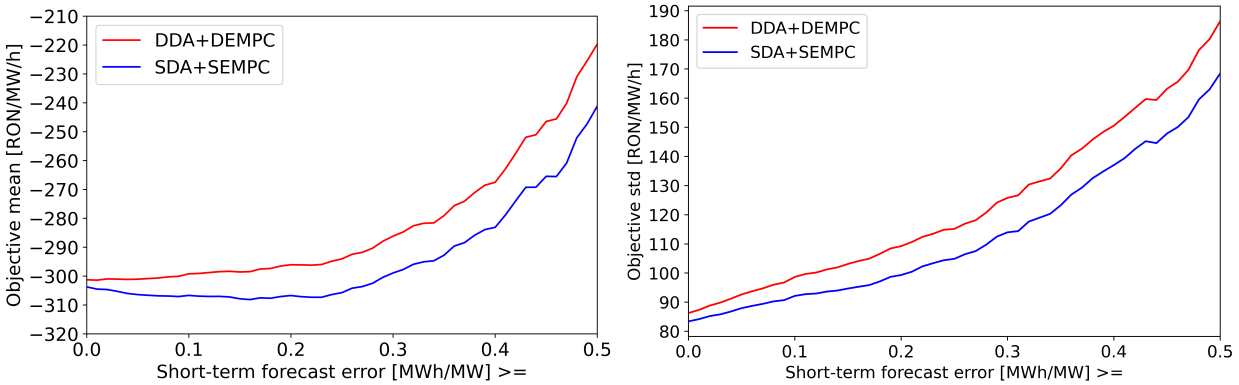

(a) Normalized ex-post mean of $\boldsymbol{J}^{\boldsymbol{DA}}$.

(b) Normalized ex-post standard deviation of $\boldsymbol{J}^{\boldsymbol{DA}}$.

Figure 7: Impact of the ST vRES energy forecast error on the mean and standard deviation of the normalized ex-post DA objective function value, i.e., ex-post value of $\boldsymbol{J}^{\boldsymbol{DA}}$. Values are in RON/MW/h since $\boldsymbol{J}^{\boldsymbol{DA}}$ is normalized by the nominal capacity of the hybrid system.

5. Discussion and conclusion

In this work, the trading and control problem of a hybrid variable vRES-BESS system participating in multiple electricity markets is addressed. First, the trading problem is addressed during the DA step, when the aggregator submits bids to the energy and balancing AS markets. Subsequently, the control problem is addressed during the ST step, where the hybrid system is controlled in near real-time to optimize the economic objectives of the aggregator.

A fully stochastic two-level architecture is proposed, incorporating stochastic programming to address the trading problem and SEMPC to handle the control problem. Subsequently, a comparison is conducted between the novel SDA+SEMPC architecture and two benchmarks employing a deterministic model to handle the uncertainty, namely DDA+DRTMPC and DDA+DEMPC. These strategies are evaluated ex-post on a real case study, using historical time series of prices and renewable power generation. The main conclusions can be summarized as follows:

1. In contrast to a traditional RTMPC approach, SEMPC directly considers the economic objectives of the aggregator in the optimization-based control strategy. This leads to higher ex-post market revenue and lower ex-post storage degradation. Under the observed price

conditions, our SDA+SEMPC successfully tracks the activation of AS without deficits in reserve provision, albeit with a modest increase in imbalances on the energy market.

2. Compared to the proposed benchmarks, which utilize deterministic models to handle uncertainty, our SDA+SEMPC exhibits lower sensitivity to vRES energy forecast errors.

The assumption of known prices is unlikely to occur in real markets. However, this modeling choice allows for a direct evaluation of the vRES energy forecast errors impact on the observed results, which is among the core objectives of this study. Moreover, our SDA+SEMPC can be easily extended to include also price forecast scenarios.

This work opens the way to further investigations in many directions, such as the provision of additional AS (e.g., voltage control), or participation in additional markets. It could be interesting to evaluate the benefits of our approach when additional sources of flexibility (e.g., controllable loads) are considered. Such an integration of additional flexibility sources could result in a very large portfolio. In this case, distributed optimization techniques could be employed to limit the computational burden.

Declaration of competing interest

The authors declare that they have no known competing financial interests or personal relationships that could have appeared to influence the work reported in this paper.

Acknowledgment

This research was carried out in part in the frame of the European project Smart4RES (Grant No. 864337), supported by the Horizon 2020 Framework Program. The authors gratefully acknowledge EDP-R, ENTSOE and ECMWF, for providing part of the dataset, and Compagnie Nationale du Rhône, for the valuable discussions.

References

[1] IEA (2022), World Energy Outlook 2022, IEA, Paris, https://www.iea.org/reports/world-energy-outlook-2022, (Last accessed April 2023) (2022).

[2] G. Rancilio, A. Rossi, D. Falabretti, A. Galliani, M. Merlo, Ancillary services markets in europe: Evolution and regulatory trade-offs, Renewable and Sustainable Energy Reviews 154 (2022) 111850. doi:https://doi.org/10.1016/j.rser.2021.111850.

[3] X. Wu, J. Zhao, A. Conejo, Optimal Battery Sizing for Frequency Regulation and Energy Arbitrage, IEEE Transactions on Power Delivery 37 (3) (2022) 2016–2023. doi:10.1109/TPWRD.2021.3102420.

[4] P. Hasanpor Divshali, C. Evens, Optimum Operation of Battery Storage System in Frequency Containment Reserves Markets, IEEE Transactions on Smart Grid 11 (6) (2020) 4906–4915. doi:10.1109/TSG.2020.2997924.

[5] C. Olk, D. U. Sauer, M. Merten, Bidding strategy for a battery storage in the german secondary balancing power market, Journal of Energy Storage 21 (2019) 787–800. doi:https://doi.org/10.1016/j.est.2019.01.019.

[6] A. Banshwar, N. K. Sharma, Y. R. Sood, R. Shrivastava, Renewable energy sources as a new participant in ancillary service markets, Energy Strategy Reviews 18 (2017) 106–120. doi:https://doi.org/10.1016/j.esr.2017.09.009.

[7] A. Michiorri, G. Lupaldi, D. Bertelli, Optimal hybrid pv-battery residential system management and sizing taking into account battery thermal behavior and ageing, in: CIRED 2020 Workshop, 2020, pp. 4–5.

[8] S. Möws, B. Wiegel, C. Becker, Day-ahead Optimization of Frequency Containment Reserve for Renewable Energies and Storage, in: 2021 IEEE PES Innovative Smart Grid Technologies Europe (ISGT Europe), 2021, pp. 1–5. doi:10.1109/ISGTEurope52324.2021.9640092.

[9] H. Pandžić, J. M. Morales, A. J. Conejo, I. Kuzle, Offering model for a virtual power plant based on stochastic programming, Applied Energy 105 (2013) 282–292. doi:https://doi.org/10.1016/j.apenergy.2012.12.077.

[10] C. A. Correa-Florez, A. Michiorri, G. Kariniotakis, Robust optimization for day-ahead market participation of smart-home aggregators, Applied Energy 229 (2018) 433–445. doi:https://doi.org/10.1016/j.apenergy.2018.07.120.

[11] G. Liu, Y. Xu, K. Tomsovic, Bidding strategy for microgrid in day-ahead market based on hybrid stochastic/robust optimization, IEEE Transactions on Smart Grid 7 (1) (2016) 227–237. doi:10.1109/TSG.2015.2476669.

[12] A. Stratigakos, S. Camal, A. Michiorri, G. Kariniotakis, Prescriptive trees for integrated forecasting and optimization applied in trading of renewable energy, IEEE Transactions on Power Systems 37 (6) (2022) 4696–4708. doi:10.1109/TPWRS.2022.3152667.

[13] S. Camal, F. Teng, A. Michiorri, G. Kariniotakis, L. Badesa, Scenario generation of aggregated Wind, Photovoltaics and small Hydro production for power systems applications, Applied Energy 242 (2019) 1396–1406. doi:https://doi.org/10.1016/j.apenergy.2019.03.112.

[14] H. Ding, P. Pinson, Z. Hu, Y. Song, Optimal offering and operating strategies for wind-storage systems with linear decision rules, IEEE Transactions on Power Systems 31 (6) (2016) 4755–4764. doi:10.1109/TPWRS.2016.2521177.

[15] S. Yumiki, Y. Susuki, Y. Oshikubo, Y. Ota, R. Masegi, A. Kawashima, A. Ishigame, S. Inagaki, T. Suzuki, Autonomous vehicle-to-grid design for provision of frequency control ancillary service and distribution voltage regulation, Sustainable Energy, Grids and Networks 30 (2022) 100664. doi:https://doi.org/10.1016/j.segan.2022.100664.

[16] J. M. Filipe, C. L. Moreira, R. J. Bessa, B. A. Silva, Optimization of the variable speed pump storage participation in frequency restoration reserve market, in: 2016 13th International Conference on the European Energy Market (EEM), 2016, pp. 1–6. doi:10.1109/EEM.2016.7521336.

[17] J. Tan, Y. Zhang, Coordinated control strategy of a battery energy storage system to support a wind power plant providing multi-timescale frequency ancillary services, IEEE Transactions on Sustainable Energy 8 (3) (2017) 1140–1153. doi:10.1109/TSTE.2017.2663334.

[18] A. González-Garrido, A. Saez-de Ibarra, H. Gaztañaga, A. Milo, P. Eguia, Annual optimized bidding and operation strategy in energy and secondary reserve markets for solar plants with storage systems, IEEE Transactions on Power Systems 34 (6) (2019) 5115–5124. doi:10.1109/TPWRS.2018.2869626.

[19] ENTSO-E (2018), An overview of the European balancing market and electricity balancing guideline, https://www.entsoe.eu/news/2018/12/12/electricity-balancing-in-europe-entso-e-releases-an-overview-of-the-european-electricity-balancing-market-and-guideline/, (Last accessed April 2023) (2018).

[20] E. F. Camacho, C. B. Alba, Model predictive control, Springer science & business media, 2013.

[21] A. González-Garrido, H. Gaztañaga, A. S. de Ibarra, A. Milo, P. Eguia, Electricity and reserve market bidding strategy including sizing evaluation and a novel renewable complementarity-based centralized control for storage lifetime enhancement, Applied Energy 262 (2020) 114591. doi:https://doi.org/10.1016/j.apenergy.2020.114591.
URL https://www.sciencedirect.com/science/article/pii/S0306261920301033

[22] Z. Chen, Z. Liu, L. Wang, A modified model predictive control method for frequency regulation of microgrids under status feedback attacks and time-delay attacks, International Journal of Electrical Power & Energy Systems 137 (2022) 107713. doi:https://doi.org/10.1016/j.ijepes.2021.107713.

[23] M. Ellis, H. Durand, P. D. Christofides, A tutorial review of economic model predictive control methods, Journal of Process Control 24 (8) (2014) 1156–1178. doi:https://doi.org/10.1016/j.jprocont.2014.03.010.

[24] F. Garcia-Torres, C. Bordons, Optimal economical schedule of hydrogen-based microgrids with hybrid storage using model predictive control, IEEE Transactions on Industrial Electronics 62 (8) (2015) 5195–5207. doi:10.1109/TIE.2015.2412524.

[25] J. R. Nelson, N. G. Johnson, Model predictive control of microgrids for real-time ancillary service market participation, Applied Energy 269 (2020) 114963. doi:https://doi.org/10.1016/j.apenergy.2020.114963.

[26] T. Zhang, H. B. Gooi, Hierarchical mpc-based energy management and frequency regulation participation of a virtual power plant, in: IEEE PES Innovative Smart Grid Technologies, Europe, 2014, pp. 1–5. doi:10.1109/ISGTEurope.2014.7028751.

[27] S. Cai, R. Matsuhashi, Model predictive control for ev aggregators participating in system frequency regulation market, IEEE Access 9 (2021) 80763–80771. doi:10.1109/ACCESS.2021.3085345.

[28] X. Ai, Z. Wu, J. Hu, Y. Li, P. Hou, Robust operation strategy enabling a combined wind/battery power plant for providing energy and frequency ancillary services, International Journal of Electrical Power Energy Systems 118 (2020) 105736. doi:https://doi.org/10.1016/j.ijepes.2019.105736.
URL https://www.sciencedirect.com/science/article/pii/S0142061519330340

[29] T. A. N. Heirung, J. A. Paulson, J. O'Leary, A. Mesbah, Stochastic model predictive control — how does it work?, Computers & Chemical Engineering 114 (2018) 158–170, fOCAPO/CPC 2017. doi:https://doi.org/10.1016/j.compchemeng.2017.10.026.

[30] F. Garcia-Torres, C. Bordons, J. Tobajas, R. Real-Calvo, I. Santiago, S. Grieu, Stochastic optimization of microgrids with hybrid energy storage systems for grid flexibility services considering energy forecast uncertainties, IEEE Transactions on Power Systems 36 (6) (2021) 5537–5547. doi:10.1109/TPWRS.2021.3071867.

[31] A. Parisio, E. Rikos, L. Glielmo, Stochastic model predictive control for economic/environmental operation management of microgrids: An experimental case study, Journal of Process Control 43 (2016) 24–37. doi:https://doi.org/10.1016/j.jprocont.2016.04.008.

[32] A. Cabrera-Tobar, A. M. Pavan, N. Blasuttigh, G. Petrone, G. Spagnuolo, Real time energy management system of a photovoltaic based e-vehicle charging station using explicit model predictive control accounting for uncertainties, Sustainable Energy, Grids and Networks 31 (2022) 100769. doi:https://doi.org/10.1016/j.segan.2022.100769.

[33] D. van der Meer, G. C. Wang, J. Munkhammar, An alternative optimal strategy for stochastic model predictive control of a residential battery energy management system with solar photovoltaic, Applied Energy 283 (2021) 116289. doi:https://doi.org/10.1016/j.apenergy.2020.116289.

[34] J. Vasilj, S. Gros, D. Jakus, M. Zanon, Day-ahead scheduling and real-time economic mpc of chp unit in microgrid with smart buildings, IEEE Transactions on Smart Grid 10 (2) (2019) 1992–2001. doi:10.1109/TSG.2017.2785500.

[35] M. Yousefi Ramandi, N. Bigdeli, K. Afshar, Stochastic economic model predictive control for real-time scheduling of balance responsible parties, International Journal of Electrical Power & Energy Systems 118 (2020) 105800. doi:https://doi.org/10.1016/j.ijepes.2019.105800.

[36] T. Borsche, F. Oldewurtel, G. Andersson, Scenario-based mpc for energy schedule compliance with demand response, IFAC Proceedings Volumes 47 (3) (2014) 10299–10304, 19th IFAC World Congress. doi:https://doi.org/10.3182/20140824-6-ZA-1003.01284.

[37] F. García-Muñoz, F. Teng, A. Junyent-Ferré, F. Díaz-González, C. Corchero, Stochastic energy community trading model for day-ahead and intraday coordination when offering der's reactive power as ancillary services, Sustainable Energy, Grids and Networks 32 (2022) 100951. doi:https://doi.org/10.1016/j.segan.2022.100951.

[38] Smart4RES: European research project supported by the Horizon 2020 Framework Program, https://www.smart4res.eu, (Last accessed April 2023).

[39] L. Meeus, The evolution of electricity markets in Europe, Edward Elgar Publishing, 2020.

[40] G. Rancilio, A. Rossi, D. Falabretti, A. Galliani, M. Merlo, Ancillary services markets in europe: Evolution and regulatory trade-offs, Renewable and Sustainable Energy Reviews 154 (2022) 111850. doi:https://doi.org/10.1016/j.rser.2021.111850.

[41] N. Naval, J. M. Yusta, Virtual power plant models and electricity markets - a review, Renewable and Sustainable

Energy Reviews 149 (2021) 111393. doi:https://doi.org/10.1016/j.rser.2021.111393.

[42] S. Camal, Forecasting and optimization of ancillary services provision by renewable energy sources, Theses, Université Paris sciences et lettres (Feb. 2020).
URL https://pastel.archives-ouvertes.fr/tel-02973808

[43] E. Namor, D. Torregrossa, F. Sossan, R. Cherkaoui, M. Paolone, Assessment of battery ageing and implementation of an ageing aware control strategy for a load leveling application of a lithium titanate battery energy storage system, in: 2016 IEEE 17th Workshop on Control and Modeling for Power Electronics (COMPEL), 2016, pp. 1–6. doi:10.1109/COMPEL.2016.7556779.